energies

MDPI

Article

Modelling of Solar Irradiance Incident on Building Envelopes in Polish Climatic Conditions: The Impact on Energy Performance Indicators of Residential Buildings

Piotr Michalak

Department of Power Systems and Environmental Protection Facilities, Faculty of Mechanical Engineering and Robotics, AGH University of Science and Technology, Mickiewicza 30, 30-059 Kraków, Poland; pmichal@agh.edu.pl; Tel.: +48-126-173-579

Abstract: In this study, we use the data of Polish typical meteorological years and 15 transposition models to obtain global solar irradiance on sloped surfaces to calculate solar irradiance on external building partitions, solar gains, heating demands, and primary nonrenewable energy for heating and domestic hot water (EP_{H+W}) of two typical Polish residential buildings, each for two variants in five locations. In relation to TMYs, annual solar gains were lower by −31% and −36% on average in a single and multifamily building, respectively, and the annual heating demands increased by 9% and 16%, respectively. Consequently, averaged EP_{H+W} in relation to TMYs rose by 1.4 kWh/m^2 and 4.5 kWh/m^2, respectively. The mean differences between TMYs and the new method from the recently published EN-ISO 52010 standard for test Building 1 were 1.6 and 1.2 kWh/m^2, for Variants 1 and 2, respectively. Similarly, for test Building 2, the mean differences were 5.1 kWh/m^2 and 3.9 kWh/m^2, respectively. This means that the simulation model that is chosen has a visible impact on a building's energy performance indicators and its rating without any changes in the physical structure and use of the building.

Keywords: typical meteorological year; solar gains; transposition model; isotropic model; anisotropic model; diffuse irradiance; heating demand; energy performance; usable energy

Citation: Michalak, P. Modelling of Solar Irradiance Incident on Building Envelopes in Polish Climatic Conditions: The Impact on Energy Performance Indicators of Residential Buildings. *Energies* **2021**, *14*, 4371. https://doi.org/10.3390/en14144371

Academic Editors: Adelio Mendes, João M. P. Q. Delgado and Ana Sofia Guimarães

Received: 11 June 2021
Accepted: 17 July 2021
Published: 20 July 2021

1. Introduction

In 2018, households in Poland were responsible for about 18% of the total national energy consumption, placing Poland above the average European share of 17% [1]; 65% of Poland's energy consumption was used for space heating. As energy prices and expenditures of households on energy carriers have been rising over recent decades, new regulations and the efficiency-related measures aimed at reduction of energy consumption in the Polish building sector [2,3] have been introduced.

The Directive on Energy Performance of Buildings (EPBD) [4] is the main legislative instrument setting energy performance standards in buildings at the European Union level. Under this Directive, the member countries applied minimum requirements regarding the energy performance of new and existing buildings and ensured the certification of their energy performance [5].

In Poland, the energy performance of buildings is defined by several indicators from which the annual demand of nonrenewable primary energy use, EP, indicated on the energy certificate, determines the energy performance level of a given building [6–8]. It depends on the calculated energy use for space heating, domestic hot water, cooling, and, in nonresidential buildings, lighting. Its maximum allowable values are set in the Ordinance of the Ministry of Infrastructure on technical conditions to be met by buildings and their locations [9]. The detailed description of the calculation procedure to obtain EP is given in the Regulation of the Minister of Infrastructure and Development on the methodology to determine the energy performance of a building and energy performance certificates [10].

For correct calculations of energy use in buildings, reliable meteorological data are essential. This is a very important issue because it is well documented that energy certificates affect the transaction prices on the retail market [11,12]. With the introduction of EPBD, files were prepared, and then published in 2008 on the Ministry of Infrastructure and Development website [13] with typical meteorological years data for 61 locations across the country.

Each file contains the basic meteorological data in hourly time steps. They include dry bulb temperature; sky temperature; relative humidity; moisture content; wind speed; wind direction; global, direct and diffuse solar irradiance on a horizontal surface; and global solar irradiance on sloped surfaces (30, 45, 60, and 90°) oriented in N, NE, E, SE, S, SW, W, and NW directions. By definition they were prepared to be used as input data for the simple hourly and, in a monthly aggregated form, for the monthly method of PN-EN ISO 13790 in order to reduce the number of time-consuming solar geometry calculations. Hence, they were, and still are willingly used in numerous simulation tools for energy auditing and energy certification of buildings. This happened regardless of the fact that, according to the authors of TMYs, several simplifications were introduced when calculating global irradiance on sloped surfaces what could result in overestimated values provided in TMYs [14]. Furthermore, in 2017, a new set of standards supporting the EPBD Directive was introduced. One new standard is EN ISO 52010–1:2017 [15] which provides the calculation procedure of solar irradiance on a surface with arbitrarily orientation and tilt. Solar irradiance affects a building's thermal balance through external walls and glazed partitions [16] influencing heating and cooling energy demand, and consequently values of energy performance indicators. Publication of the EN ISO 52010 standard means that values of the global solar irradiance in the Polish typical meteorological years data should be recalculated to assess the differences between values currently used and those provided by the new method.

Therefore, the question arises, "To what extent an application of various simulation models to obtain global solar irradiance on sloped surfaces may influence calculated solar gains and resulting heating demands of buildings being the base for preparation of the energy certificate?"

2. Literature Review

In general, the basic variables concerning solar radiation measured in meteorological stations are global horizontal, direct beam, and diffuse horizontal irradiance; however, in practice, sloped and vertical surfaces are usually found (walls, roof, solar collectors, PV panels, etc.). Therefore, calculations of solar irradiance on sloped surfaces basedon solar data from measurements has been an important scientific problem resulting in the development of different transposition models over the last few decades [17,18]. Numerous studies on performance of these models against measurements performed around the world have also been published. Some of these models have also been used in Polish conditions. Chwieduk [19] applied one isotropic (Liu-Jordan) and one anisotropic (HDKR) model to determine available solar energy on a building envelope in Warsaw. Hourly sums of global and diffuse solar irradiance, measured at the Warsaw-Bielany actinometric station during the 1971–2000 period, were used. The author concluded that the isotropic model underestimated solar radiation on a building envelope and the anisotropic model must be used in a building's thermal calculations.

In addition, several studies have attempted to find an accurate model for Polish climate conditions. In [20], an analysis based on a four-year measurement database from the actinometric station in Wrocław (south-west Poland) was performed using 14 models. The root mean square error (RMSE) in percent among TMY datasets and modelled global solar irradiance on an inclined surface varied from 33.6% to 40.6% and from 29.2% to 38.5% for angles of 35° and 50°, respectively. The best results were obtained by the anisotropic Reindl model, and then by Gueymard, Perez, Koronakis, and Muneer models. In [21], the 12-year time series of measured solar radiation for Belsk in central Poland was converted

according to the ISO 15927-4 standard and the TMY3 method, and then compared with a TMY. The RMSE related to the TMY was greater than 5%. A comparison of seven models based on measurements and the TMY for Poznań in central-west Poland was presented in [22]. The best accuracies were obtained for the Koronakis and Hay models.

Heating and cooling energy consumption of a building results from thermal balance governing heat gains and losses [23] and may be lowered using solar energy. Recently, different methods to control solar energy flow in connection with a building's energy performance have been presented, such as windows with different thermal (U) and solar energy (g) transmittances [24,25], shading strategies [26], and inclination angles of windows [27].

Chwieduk [28] analysed the annual distribution of energy for heating and cooling of a hypothetic room with a single north-, south-, east-, or west-oriented window, located in Warsaw (central Poland). Different sizes, slopes, and azimuth angles were chosen. Solar irradiance was calculated using the HDKR model. A similar study on the daily distribution of heating and cooling energy was presented in [29]. In all cases, heating demand depended significantly on solar gain and was highest and lowest for the north and south-oriented window, respectively.

In other studies, authors have studied the impact of different factors on annual energy use in buildings as the window-to-wall ratio (WWR) [30] or building shape and U-values of envelope elements [31] but an influence of the various models of solar irradiance incident on external partitions on the obtained results have not been investigated. We found only a few papers that have been dedicated to this issue.

In [32], solar irradiance on an envelope of a multifamily building in Kraków (south Poland) was computed by five models (Hay, Muneer, Reindl, Perez, and EN ISO 52010-1). The differences in annual heating demands, calculated using the monthly method of EN ISO 13790 related to the TMY, were up to 10%.

In [33,34], a set of 22 horizontal diffuse irradiance decomposition (separation) models along with 12 irradiance models for tilted surfaces (Liu and Jordan, Temps and Coulson, Burgler, Klucher, Hay and Davies, Skartveit and Olseth, Reindl, Ma and Iqbal, Gueymard, Perez, and two models by Muneer) which resulted in 264 combinations that were considered. Then, simulations of heating and cooling demands in five European cities were performed on a set of 72 simplified buildings. On the one hand, the authors revealed that heating needs indicated little dependence (measured by the Pearson's index) on the choice of irradiance models. This impact was greater in buildings with low heating needs, especially low energy objects. On the other hand, cooling needs were significantly affected by the choice of the solar models.

The presented review shows an application of various mathematical models to obtain solar irradiance on inclined surfaces from measurements or TMYs. These models were also intensively compared with measurements at numerous locations around the world. Different technical factors influencing solar gains and thermal balance in buildings were also investigated. However, there is a lack of studies on the impact of the choice of the model of diffuse irradiance incident on a tilted surface on solar gains and heating demands of buildings; therefore, this problem is the main objective of this study.

For this purpose, hourly direct and diffuse horizontal irradiance data from measurements were taken from TMYs for five locations in Poland and were used to calculate solar irradiance on sloped surfaces using 15 different transposition models (isotropic, pseudo-isotropic, and anisotropic). The calculation procedure to obtain hourly zenith and incidence angles was taken from EN ISO 52010-1. Then, the annual energy demands for space heating in two exemplary residential buildings were calculated using the monthly method from the EN ISO 13790 standard. All results were compared with values computed using Polish TMYs.

The location, climatic, and solar conditions of Poland and Polish typical meteorological years are described in Section 3. In Section 4, we show a calculation procedure to obtain the hourly position of the Sun and briefly present 15 transposition models used to predict

global solar irradiance on sloped surfaces. In Section 5, we show, in detail, the calculation assumptions and the test buildings. A discussion of the results is presented in Section 6 and then final conclusions are provided.

3. Polish Typical Meteorological Years

Poland is located in Central Europe between 49° and 54.5° of northern latitude and from 14.1° to 24.1° of eastern longitude. The climate of Poland is moderate with marine and continental influences. The average annual sunshine duration in Poland is about 1600 h, which varies in different parts of the country. Greater and lesser values are noticed in the northern and southeast part of Poland, respectively [35].

Sunshine duration also varies throughout the year and is approximately 25% and 75% of the total annual value for the cold (X–III) and warm (IV–IX) half years, respectively. Average annual solar irradiation on a horizontal surface is in the range from 950 kWh/m^2 in the northern part of the country to 1250 kWh/m^2 in the central and eastern regions and northern coastal belt [36–38]. It varies during a year in a form similar to sunshine duration. For example, in Kołobrzeg (near the Baltic Sea), for the observation period from 1963 to 2014, the average irradiation in the cold half year was 19% of its total annual value [39].

Although Poland has less favourable solar conditions than countries of southern Europe [40], the available solar energy is sufficient to use it in building applications [41–43] and it has an important share in the thermal balance of Polish buildings [44,45].

The typical meteorological years, which are freely available for the area of Poland [13,46], were developed in 2004, using the source meteorological datasets from long-term measurements conducted by the Institute of Meteorology and Water Management (Polish abbreviation, IMGW). They contained data from 1971 to 2000 for meteorological stations with continuous three-hour measurements and observations, taken hourly or every three hours per day and coded following the SYNOP FM-12 key, for a period of at least 10 years for 61 stations. For 43 stations, the lengths of the measurement periods were continuous 30-year sequences and, for the remaining 19 stations, the lengths of measurement periods ranged from 11 to 29 years, but these were not always consecutive calendar years.

During the data processing, annual or monthly sequences with long periods of discontinuity or lack of meteorological observations were rejected. In the case of observational data with eight times a day or shorter interruptions of several hours to obtain hourly values, the source data were interpolated with the use of third degree spline curves [14,47–49].

Files with typical meteorological years in hourly and monthly formats have been prepared and are available for 61 weather stations [13,46]. Each file has the header line including information about the type of meteorological data (iso, wec, tmy, try, cwy, and hsy), code (number) and name of the World Meteorological Organization (WMO) station, north latitude, east longitude, height above sea level, time zone from 0 to east, number of days of meteorological data, and the version number of a file. The second line contains column headers (Table 1) for meteorological data. The next 8760 lines are weather data for consecutive hours of the year, starting on 1 January (Monday). The monthly weather files have 12 weather data lines.

Due to the fact that in Poland not all meteorological stations performed actinometric measurements, the source weather data on solar irradiance, in some cases, could also be computed from other meteorological parameters. Unfortunately, there are no additional data about the data processing and conversion procedures used. Regardless of this, hourly values of global, direct and diffuse solar irradiance on a horizontal surface given in TMYs are reliable data because they come from a well-known source and established and commonly accepted procedures were used for the measurements.

Table 1. The description of the data record in files with typical meteorological years (I—integer; F—float) [13,46,50].

Field Number	Name (Symbol)	Unit	Format
1	Number of the hour (N)	—	I2
2	Month (M)	—	I2
3	Day (D)	—	I2
4	UTC (GMT Greenwich Mean Time) (H)	—	I2
5	Dry bulb temperature (DBT)	°C	I5.1
6	Relative humidity (RH)	%	I2
7	Moisture content (HR)	g/kg	F6.3
8	Wind speed (WS)	m/s	F4.1
9	Wind direction (WD) in 36 sectors: 0—silence, N—36, E—9, S—18, W—27, etc. 99—variable		I2
10	Global solar irradiance on a horizontal surface (ITH)	W/m^2	F5.1
11	Direct solar irradiance on a horizontal surface (IDH)	W/m^2	F5.1
12	Diffuse solar irradiance on a horizontal surface (ISH)	W/m^2	F5.1
13	Sky temperature (TSKY)	°C	F5.2
14	Total solar radiation intensity on the horizontal surface (direction N inclination 0°) (N_0)	W/m^2	F5.1
15–47	Global solar irradiance on surfaces with N, NE, E, SE, S, SW, W, NW orientation and slope angle of 30°, 45°, 60°, 90° (N_30, NE_30, . . .)	W/m^2	F5.1

4. Modelling of Solar Irradiance on Sloped Surfaces

4.1. Introduction

The calculation procedure presented in this section was taken from EN ISO 52010-1 [15,51] to establish the same base for further comparisons. To obtain solar irradiance on a sloped surface in a given location, first, several additional variables should be calculated. The solar declination is given by the formula:

$$\delta = 0.33281 - 22.984 \cdot \cos(B) - 0.3499 \cdot \cos(2B) - 0.1398 \cdot \cos(3B) + 3.7872 \cdot \sin(B) + 0.03205 \cdot \sin(2B) + 0.07187 \cdot \sin(3B), \quad (1)$$

where:

$$B = 360 \cdot n_{day}/365. \quad (2)$$

Solar time (t_s) is determined from:

$$t_s = (n_{hour} - t_{eq})/(60 - T_{shift}), \quad (3)$$

where:

$$T_{shift} = TZ - \lambda_w/15. \quad (4)$$

TZ is the time zone for the latitude of a meteorological station (λ_w). Daylight saving time is disregarded.

The equation of time (t_{eq}) is expressed as:

$$\begin{gathered} t_{eq} = 2.6 + 0.44 \cdot n_{day}, \text{ if } n_{day} < 21, \\ t_{eq} = 5.2 + 9.0 \cdot \cos[(n_{day} - 43) \cdot 0.0357 \cdot 180/\pi] \text{ if } 20 \leq n_{day} < 136, \\ t_{eq} = 1.4 - 5.0 \cdot \cos[(n_{day} - 135) \cdot 0.0449 \cdot 180/\pi] \text{ if } 136 \leq n_{day} < 241, \\ t_{eq} = -6.3 - 10.0 \cdot \cos[(n_{day} - 306) \cdot 0.036 \cdot 180/\pi] \text{ if } 241 \leq n_{day} < 336, \\ t_{eq} = 0.45 \cdot (n_{day} - 359) \text{ if } n_{day} \geq 336, \end{gathered} \quad (5)$$

The solar hour angle ω is calculated in the middle of a given hour:

$$\omega = 15 \cdot (12.5 - t_s), \tag{6}$$

From the above, the solar altitude angle can be obtained as follows:

$$\alpha_{sol} = \arcsin\left(\sin(\delta) \cdot \sin(\varphi_w) + \cos(\delta) \cdot \cos(\varphi_w) \cdot \cos(\omega)\right), \tag{7}$$

and the zenith angle:

$$\theta_z = 90 - \alpha_{sol}. \tag{8}$$

The azimuth angle is measured from the south with a positive sign in the east direction. Knowing the slope angle of a surface (β) and the azimuth angle (γ), the angle of incidence can be calculated as follows:

$$\begin{aligned} \theta = \arccos\,[&\sin(\delta) \cdot \sin(\varphi_w) \cdot \cos(\beta) - \sin(\delta) \cdot \cos(\varphi_w) \cdot \sin(\beta) \cdot \cos(\gamma) + \\ &\cos(\delta) \cdot \cos(\varphi_w) \cdot \cos(\beta) \cdot \cos(\omega) + \cos(\delta) \cdot \sin(\varphi_w) \cdot \sin(\beta) \cdot \cos(\gamma) \cdot \cos(\omega) + \\ &\cos(\delta) \cdot \sin(\beta) \cdot \sin(\gamma) \cdot \sin(\omega)]. \end{aligned} \tag{9}$$

4.2. Global Irradiance on a Sloped Surface

In general, global irradiance on a sloped surface is the sum of beam (direct), diffuse, and reflected components:

$$I_{g,s} = I_{b,s} + I_{d,s} + I_{r,s}. \tag{10}$$

The transposition model predicts global irradiance from input (measured and/or modelled) components of horizontal irradiance:

$$I_{g,s} = I_{b,h} \cdot R_b + I_{d,h} \cdot R_d + (I_{b,h} + I_{d,h}) \cdot \rho \cdot R_r, \tag{11}$$

where:

$$R_b = \cos\theta / \cos\theta_z. \tag{12}$$

The ground reflected component is commonly assumed to be isotropic:

$$R_r = (1 - \cos\beta)/2. \tag{13}$$

The diffuse component is given by:

$$I_{d,s} = I_{d,h} \cdot R_d. \tag{14}$$

The diffuse transposition factor, R_d, can be calculated from various transposition models developed over the last few decades. Several reviews presenting these models have been published recently [52–55]. A study of Yang [56] also showed several identified errors in models found in the literature.

In this study, besides data from TMYs, 15 transposition models were used, as follows: isotropic (Liu-Jordan—Model 1, Badescu—Model 2), pseudo-isotropic (Koronakis—Model 3) and anisotropic (Circumsolar—Model 4, Bugler—Model 5, Klucher—Model 6, Hay—Model 7, Willmott—Model 8, Ma and Iqbal—Model 9, Skartveit and Olseth—Model 10, Reindl—Model 11, Gueymard—Model 12, Muneer—Model 13, Perez—Model 14, and Perez described in EN ISO 52010—Model 15). They are briefly presented in the following subsections.

4.3. Transposition Models

4.3.1. TMY

In the files with TMYs, data for hourly global solar irradiance calculated (not measured) for eight basic geographic directions and five slope angles were also provided. According to [46–48], they were computed using a simple mathematical model assuming that the diffuse solar radiation reaches each plane from the entire hemisphere. The reflec-

tion and scattering of solar radiation by the ground and the building's surroundings were not accounted for, hence, global solar irradiance on a sloped surface in that model is given in the form:

$$I_{g,s} = I_{b,h} \cdot R_b + I_{d,h}. \quad (15)$$

However, in energy simulations of buildings, the reflected component of solar radiation is considered. Therefore, this component was also included in all studied models. Ground and surroundings reflectance of $\rho = 0.2$ was used as commonly adopted in this type of calculations [57].

4.3.2. Liu-Jordan

This model was firstly introduced by Kondratyev and Manolova [58] but is known as the Liu–Jordan model [59] as follows:

$$R_d = (1 + \cos\beta)/2. \quad (16)$$

4.3.3. Badescu

The Badescu model [60] is described as:

$$R_d = (3 + \cos(2\beta))/4. \quad (17)$$

4.3.4. Koronakis

The Koronakis model [61] is described as:

$$R_d = (2 + \cos\beta)/3. \quad (18)$$

4.3.5. Circumsolar

This model was described by Iqbal [62] as follows:

$$R_b = R_d = \cos\theta/\cos\theta_z. \quad (19)$$

4.3.6. Bugler

The Bugler model [63] is described as:

$$R_d = (1 - 0.05 \cdot I_{b,h}/I_{d,h})\,(1 + \cos\beta)/2 + 0.05 \cdot I_{b,n} \cdot \cos\theta/I_{d,h}. \quad (20)$$

Direct normal irradiance is given by:

$$I_{b,n} = I_{b,h}/\sin(\alpha_{sol}). \quad (21)$$

4.3.7. Klucher

The Klucher model [64] is described as:

$$R_d = 0.5\,(1 + \cos\beta)\,(1 + F \cdot \sin^3(\beta/2))\,(1 + F \cdot \cos^2\theta \cdot \sin^3\theta_z), \quad (22)$$

where:

$$F = 1 - (I_{d,h}/I_{g,h})^2. \quad (23)$$

4.3.8. Hay

The Hay model [65] is described as:

$$R_d = k_H\, R_b + 0.5\,(1 + \cos\beta)\,(1 - k_H), \quad (24)$$

where:

$$k_H = I_{d,n}/G_{sol,c}. \quad (25)$$

4.3.9. Willmott

The Willmott model [66] is described as:

$$R_d = k_H R_b + 0.5 \cdot C_\beta \cdot (1 - k_H), \quad (26)$$

where:

$$C_\beta = 1.015 - 0.20293\ \beta - 0.080823\ \beta^2, \quad (27)$$

for β given in radians.

4.3.10. Ma and Iqbal

The Ma and Iqbal model [67] is described as:

$$R_d = k_T R_b + 0.5\ (1 + \cos\beta)\ (1 - k_T). \quad (28)$$

$$k_T = I_{g,h}/I_{ext}, \quad (29)$$

where:

$$I_{ext} = G_{sol,c} \cdot [1 + 0.033 \cdot \cos(360 \cdot n_{day}/365)]. \quad (30)$$

4.3.11. Skartveit and Olseth

The Skartveit and Olseth model [68] is described as:

$$R_d = k_D R_b + Z \cos\beta + 0.5\ (1 + \cos\beta)\ (1 - k_D - Z) \quad (31)$$

where:

$$Z = \max\ (0, 0.3 - 2k_H), \quad (32)$$

$$k_D = (I_{g,h} - I_{d,h})/I_{ext,h}, \quad (33)$$

$$I_{ext,h} = I_{ext} \cdot \sin\alpha_{sol}. \quad (34)$$

4.3.12. Reindl

The Reindl model [69] is described as:

$$R_d = k_D R_b + 0.5\ (1 + \cos\beta)\ (1 - k_D)\ (1 + k_R \sin^3(\beta/2)) \quad (35)$$

where:

$$k_R = \sqrt{I_{b,h}/I_{g,h}} \quad (36)$$

4.3.13. Gueymard

The Gueymard model [70] is described as:

$$R_d = (1 - N_{pt})\ R_{d,0} + N_{pt}\ R_{d,1}, \quad (37)$$

where:

$$R_{d,0} = \exp(a_0 + a_1 \cos\theta + a_2 \cos^2\theta + a_3 \cos^3\theta) + F(\beta)\ G(\alpha_{sol}), \quad (38)$$

$$R_{d,1} = \frac{1 + \cos\beta}{2} + \frac{2b}{\pi(3 + 2b)}\left(\sin\beta - \beta\cos\beta - \pi\left(\sin\frac{\beta}{2}\right)^2\right), \quad (39)$$

$$a_0 = -0.897 - 3.364\ h' + 3.960\ h'^2 - 1.909\ h'^3, \quad (40)$$

$$a_1 = 4.448 - 12.962\ h' + 34.601\ h'^2 - 48.784\ h'^3 + 27.511\ h'^4, \quad (41)$$

$$a_2 = -2.770 + 9.164\ h' - 18.876\ h'^2 + 23.776\ h'^3 - 13.014\ h'^4, \quad (42)$$

$$a_3 = 0.312 - 0.217\ h' - 0.805\ h'^2 + 0.318\ h'^3, \quad (43)$$

$$F(\beta) = (1 + b_0 \sin^2(\beta) + b_1 \sin(2\beta) + b_2 \sin(4\beta))/(1 + b_0), \quad (44)$$

$$G(\alpha_{sol}) = 0.408 - 0.323\,h' + 0.384\,h'^2 - 0.170\,h'^3, \quad (45)$$

$$H' = 0.01\alpha_{sol} \text{ (in degrees)}, \quad (46)$$

and $b_0 = 0.2249$, $b_1 = 0.1231$, and $b_2 = 0.0342$.

Also:

$$N_{pt} = \max\{\min(Y, 1), 0\}, \quad (47)$$

where:

$$Y = 6.667 \cdot I_{d,h}/I_{g,h} - 1.4167 \text{ if } I_{d,h}/I_{g,h} \leq 0.227, \quad (48)$$

otherwise:

$$Y = 1.2121 \cdot I_{d,h}/I_{g,h} - 0.1758. \quad (49)$$

4.3.14. Muneer

The Muneer model [71] is described as:

$$R_d = k_D\,R_b + (1 - k_D)\,[\cos^2(\beta/2) + (2b/(\pi\,(3 + 2b))\,(\sin\beta - \beta\,\cos\beta - \pi\,\sin^2(\beta/2))], \quad (50)$$

for β in radians.

For Northern Europe (where Poland lies):

$$2b/(\pi\,(3 + 2b)) = 0.00333 - 0.415\,k_H - 0.6987\,{k_H}^2. \quad (51)$$

4.3.15. Perez

We used the most widely known version of the Perez model [56] taken from [72]. This model is described as:

$$R_d = 0.5\,(1 + \cos\beta)\,(1 - F_1) + F_1 \cdot a/b + F_2\,\sin\beta, \quad (52)$$

The model coefficients (a and b), sky's clearness ε and sky's brightness Δ are given by the following relationships, respectively:

$$a = \max[0; \cos(\theta)], \quad (53)$$

$$b = \max[\cos(85^\circ); \cos(\theta_z)], \quad (54)$$

$$\varepsilon = \frac{\frac{I_{d,h}+I_{b,n}}{I_{d,h}} + 1.041\left(\frac{\pi}{180}\theta_z\right)^3}{1 + 1.041\left(\frac{\pi}{180}\theta_z\right)^3}, \quad (55)$$

$$\Delta = m \cdot I_{d,h}/I_{ext}. \quad (56)$$

The optical air mass is calculated using the formula given in [15]. If $\alpha_{sol} < 10$, then:

$$m = 1/(\sin(\alpha_{sol}) + 0.15 \cdot (\theta + 3.885)^{-1.253}), \quad (57)$$

elsewhere:

$$m = 1/\sin(\alpha_{sol}). \quad (58)$$

Circumsolar (F_1) and horizon brightness (F_2) coefficients are given by:

$$F_1 = \max[0; f_{11}(\varepsilon) + f_{12}(\varepsilon) \cdot \Delta + f_{13}(\varepsilon) \cdot (\pi \cdot \theta_z/180)], \quad (59)$$

$$F_2 = f_{21}(\varepsilon) + f_{22}(\varepsilon) \cdot \Delta + f_{23}(\varepsilon) \cdot (\pi \cdot \theta_z/180). \quad (60)$$

In each calculation, the time step values of coefficients $f_{11} \ldots f_{23}$ are dependent on a sky's clearness ε and can be derived from Table 2.

Table 2. Coefficients $f_{11}, \ldots, f_{23}$.

ε	f_{11}	f_{12}	f_{13}	f_{21}	f_{22}	f_{23}
<1.065	−0.008	0.588	−0.062	−0.060	0.072	−0.022
<1.23	0.130	0.683	−0.151	−0.019	0.066	−0.029
<1.5	0.330	0.487	−0.221	0.055	−0.064	−0.026
<1.95	0.568	0.187	−0.295	0.109	−0.152	−0.014
<2.8	0.873	−0.392	−0.362	0.226	−0.462	−0.001
<4.5	1.132	−1.237	−0.412	0.288	−0.823	0.056
<6.2	1.060	−1.600	−0.359	0.264	−1.127	0.131
≥6.2	0.678	−0.327	−0.250	0.156	−1.377	0.251

4.3.16. EN ISO 52010

The EN ISO 52010 standard uses the same Perez model [15]. But the equation describing sky clearness was given there in the form:

$$\varepsilon = \frac{\frac{I_{d,h}+I_{b,n}}{I_{d,h}} + 1.014\left(\frac{\pi}{180}\alpha_{sol}\right)^3}{1 + 1.014\left(\frac{\pi}{180}\alpha_{sol}\right)^3}. \quad (61)$$

The zenith angle (compare Equation (55)) was changed with the solar altitude angle, and the coefficient 1.041 was changed to 1.014.

5. Materials and Methods

5.1. Test Buildings

For the purposes of thermal calculations of buildings, Poland is divided according to the PN-EN 12831 standard [73–75] into five climate zones (Figure 1), according to the design outside temperature from −16 °C in Zone I, the warmest zone, to −20 °C in Zone V, the coldest zone, defined in the standard (Table 1).

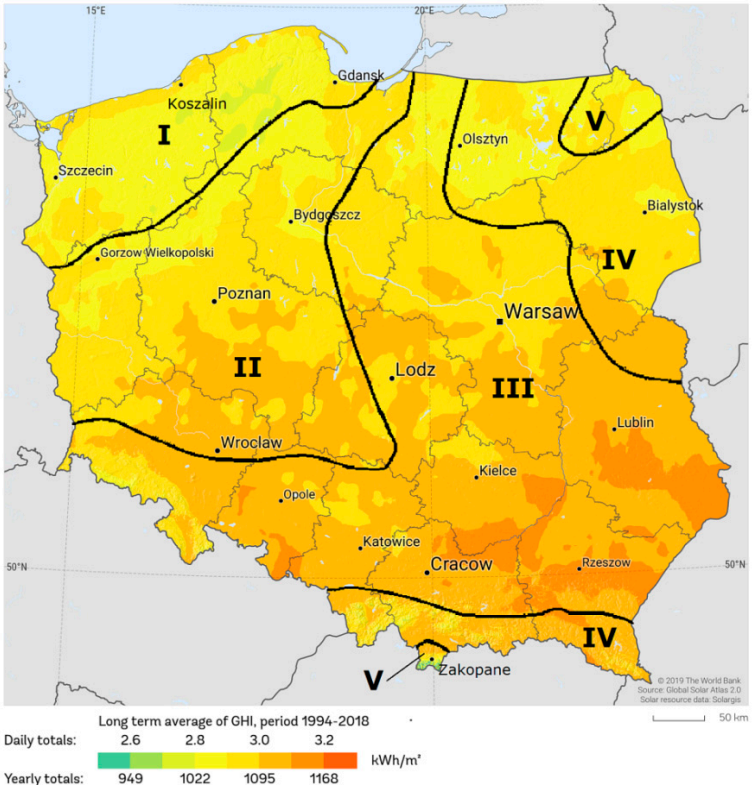

Figure 1. Climatic zones of PN-EN 12831 [73] and global annual solar irradiation on a horizontal surface in Poland [76].

For 42 of the 61 meteorological stations in Poland, the TMY source datasets have full 30-year (1971–2000) measurement periods. Among them, five locations (Table 3) were chosen for further analysis, one in each of five climatic zones of Poland numbered according to PN-EN 12831. For clarity, they were numbered with Roman numerals as in Figure 1. The annual irradiation was taken from the TMYs. The CDD and HDD (base temperature of 18.3 °C) are given in the EnergyPlus weather database [77]. A more detailed description of climatic conditions in the selected locations is given in Figure 2 (monthly air temperature variation) and in Figure 3 (monthly solar irradiation on a horizontal surface). Typical meteorological years for the considered locations in hourly format were taken from [13] and were given in Supplementary Material S1.

Table 3. Test locations.

No.	1	2	3	4	5
Locations	Koszalin	Poznań	Kielce	Białystok	Zakopane
Climate zone	I	II	III	IV	V
Design outside temperature (°C)	−16	−18	−20	−22	−24
Mean annual temperature (°C)	8.0	8.2	7.5	6.9	5.4
Altitude (m)	0	92	261	151	857
H (kWh/m^2)	827.4	960.8	981.1	897.1	1006.7
CDD	63	114	74	63	19
HDD	3716	3621	4002	4168	4585
Latitude	54°12′ N	52°25′ N	50°49′ N	53°06′ N	49°18′ N
Longitude	16°09′ E	16°51′ E	20°42′ E	23°10′ E	19°58′ E

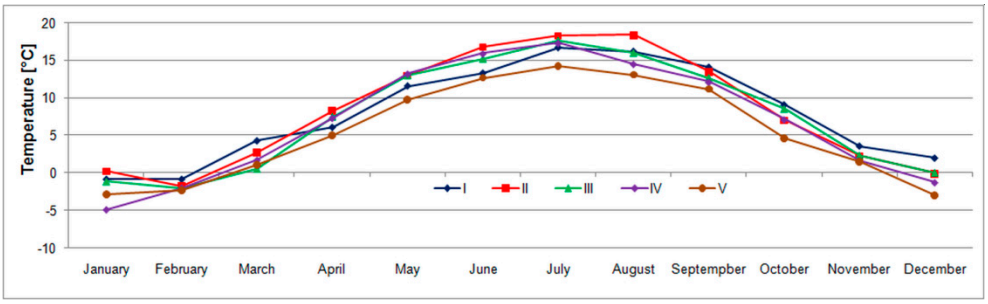

Figure 2. Monthly air temperature in the considered locations.

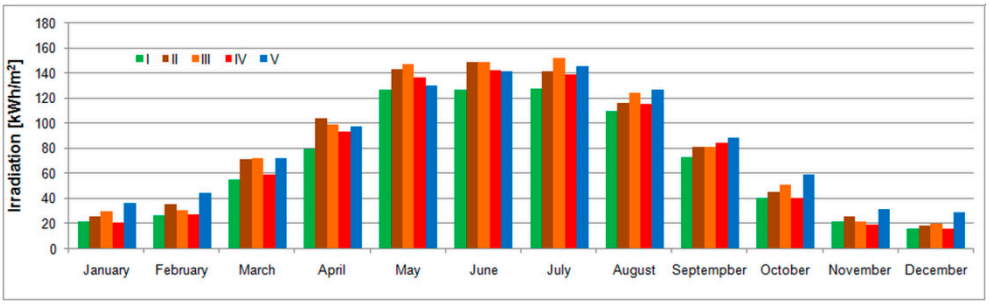

Figure 3. Monthly irradiation in the considered locations.

To evaluate the impact of different transposition models (Section 4) on calculated solar gains and heating demands, we used two typical Polish residential buildings described in the TABULA project [78] dedicated to the energy-performance related calculations of buildings [79]. Because Poland is a country with a heating dominated climate [80–82] both buildings were with no cooling. The first building (Figure 4a) is a single-family one-story house with an attic and a gable roof (inclined at 30°). The second building (Figure 4b) is a multifamily five-storey building with a nonheated basement and a flat roof.

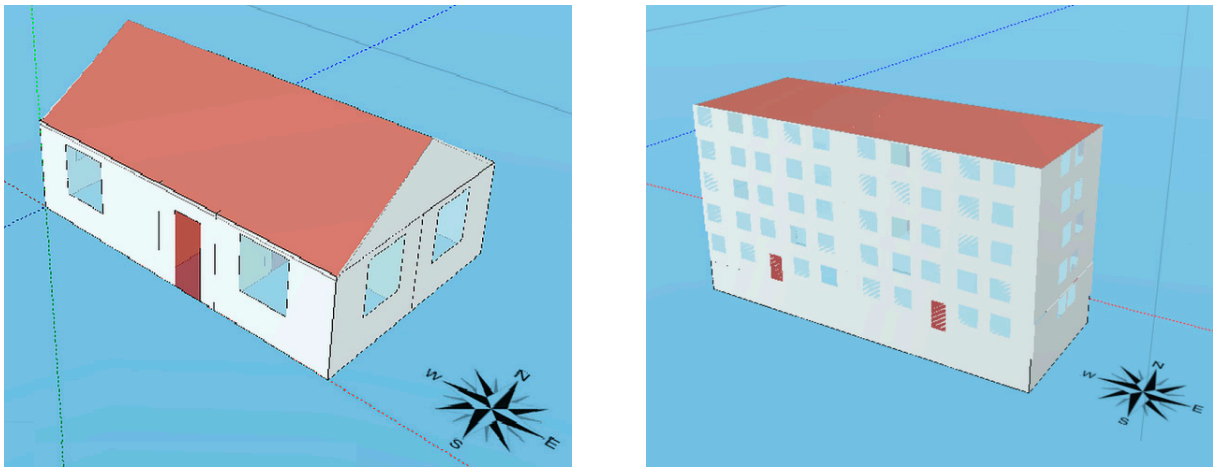

(**a**) (**b**)

Figure 4. Models of the test buildings in the Audytor OZC program: (**a**) Single-family building; (**b**) multifamily building.

The buildings both fulfill requirements described in the Polish regulations concerning energy performance of newly built buildings since 1 January 2017 [82], at the time of the new standard introduction.

The thermal parameters of the buildings were obtained from the Audytor OZC tool. It is a simulation program commonly used in energy certification of buildings in Poland. Its main features have been described in [83–85].

Several parameters are identical in both cases; external walls and the roof have $\alpha_{op} = 0.6$ and $\alpha_{op} = 0.9$, respectively. PVC windows and glazed balcony doors with the frame factor $F_F = 0.3$ (area of frames and dividers in the total area of windows or glazed doors) were used.

Internal gain densities per floor area, efficiencies of heating systems, domestic hot water use, and working time of circulating pumps were taken from [10]. No shading was assumed. Heat sources are typical in Polish buildings [86,87]. In Building 1 for domestic hot water, preparation solar collectors are used with a gas boiler with 50% share, as well founded in Polish conditions [88,89]. The main geometric and thermal parameters of both buildings are given in Table 4.

To see how the energy indicators may scale with different building parameters, in terms of the presented analysis, twovariants, i.e., area of windows (window-to-wall ratio (WWR)) and solar energy transmittance of windows and balcony doors (Table 5), were applied as the main parameters influencing solar gains through glazed partitions [90]. In the second building, the area of windows variant was also reduced.

In Poland, the monthly quasi-steady-state method of EN ISO 13790 [91] is used in energy auditing and energy certification of buildings [92,93] and this method was used in the calculations.

Table 4. Physical parameters of test buildings.

Parameter	Building 1	Building 2	Unit
Length	10.5	29.5	m
Width	7.0	11.0	m
Height above the ground	2.7	14.7	m
Total heated area	71.4	1515.0	m^2
Total heated volume	357.0	3787.5	m^3
Number of inhabitants	5	120	—
Heat transfer coefficient by ventilation (H_{ve})	60.81	645.19	W/K
Internal heat capacity C_m	23.56	393.90	MJ/K
Internal gains density per floor area	6.8	5.9	W/m^2
Ventilation airflow	178.5	1894.0	m^3/h
External wall area—N	38.9	433.6	m^2
External wall area—S	38.9	433.6	m^2
External wall area—E	32.9	161.7	m^2
External wall area—W	32.9	161.7	m^2
Area of the roof	86.0	324.5	m^2
Thermal transmittance of external walls	0.227	0.218	W/m^2K
Thermal transmittance of the roof	0.165	0.155	W/m^2K
Thermal transmittance of the floor on the ground	0.221	0.330	W/m^2K
Thermal transmittance of windows and glazed doors	1.1	1.1	W/m^2K
Thermal transmittance of external doors	1.5	1.5	W/m^2K
Heat source (heating)	Condensing gas boiler	Heating network	—
Heat source (hot water)	Condensing gas boiler + solar collectors	Heating network	—
Average annual total efficiency of the heating system, $\eta_{H,tot}$	0.84	0.88	—
Average annual total efficiency of the domestic hot water heating system, $\eta_{w,tot}$	0.61	0.85	—
Circulating pump power, heating	50	1500	W
Circulating pump power, hot water	30	0	W

Table 5. Physical parameters of test buildings (WT2017).

Parameter	Building 1		Building 2		Unit
	Variant 1	Variant 2	Variant 1	Variant 2	
Heat transfer coefficient by transmission (H_{tr})	111.47	107.80	756.0	704.8	W/K
WWR—N	6.2	4.9	23.9	20.8	%
WWR—S	17.4	13.9	20.1	16.1	%
WWR—E	24.6	21.9	25.0	17.1	%
WWR—W	14.1	11.3	25.0	17.1	%
WWR—roof	5.6	4.5	0.0	0.0	%
Solar energy transmittance of windows and glazed doors (g_{gl})	0.75	0.50	0.75	0.50	—

5.2. Calculation of Solar Gains

The calculation procedure is briefly presented here to visualize how the elements influence the value of solar heat gains in a building. If the effect of shading is not considered, the overall solar heat gains for a single thermal zone result from solar radiation in the concerned locality, orientation, solar transmittance, absorption, and the thermal heat transfer characteristics of collecting areas. A thermal characteristic and area of a collecting surface are included in an effective solar collecting area.

The heat flow by solar gains through a building element is given by:

$$\Phi_{sol} = F_{sh,ob} \cdot A_{sol} \cdot I_{tot} - F_{sky} \cdot \Phi_r. \quad (62)$$

The calculation of the effective solar collecting area depends on the kind of an element. For a glazed element (e.g., a window), it is given by:

$$A_{sol} = F_{sh,gl} \cdot g_{gl} \cdot (1 - F_F) \cdot A_c. \quad (63)$$

For an opaque element, the effective solar collecting area is given by:

$$A_{sol} = \alpha_{op} \cdot R_{se} \cdot U_c \cdot A_c. \quad (64)$$

The extra heat flow due to thermal radiation to the sky is actually not a solar heat gain, but it was included in the standard for solar gains for convenience. This heat flow for a specific building envelope element is calculated from:

$$\Phi_r = R_{se} \cdot U_c \cdot A_c \cdot h_{r,e} \cdot \Delta\theta_{sky} \quad (65)$$

The average difference between the external air temperature and the apparent sky temperature, $\Delta\theta_{sky}$, can be obtained from both these components provided in TMYs. Sky temperature is used to describe long wave radiative heat exchange between the ground or external surfaces of buildings and the sky. For this purpose, the sky is assumed to be a blackbody at some equivalent temperature known as the sky temperature. Its value depends on atmospheric conditions.

Solar gain in the i-th month is calculated as:

$$Q_{sol,i} = \Phi_{sol} \cdot \Delta\tau_m \quad (66)$$

Annual solar gain is calculated as:

$$Q_{sol} = \sum_{i=1}^{i=12} Q_{sol,i} \quad (67)$$

5.3. Energy Performance Indicators

In addition to solar gains, two indicators of buildings' energy performance were calculated. The first indicator is the heating energy need per conditioned floor area (E_A). Its annual values of 15 and 40 kWh/m^2 were established in 2012 as the maximum allowable by Polish National Fund for Environmental Protection and Water Management for passive and low energy buildings, respectively [94–96]. In the Polish regulations concerning energy certification in residential buildings, this indicator is called EU—usable energy [97].

In addition, the primary annual energy for heating and domestic hot water indicator, EP_{H+W}, was calculated.

According tothe Ordinance of the Minister of Infrastructure on technical conditions to be met by buildings and their locations [98], a building and its heating, ventilation, air-conditioning, hot water systems, and in the case of public utility buildings, collective residence, production, utility, and warehouse buildings, also built-in lighting should be designed and constructed in a way that ensures that the following minimum requirements are met:

- The value of the annual demand for nonrenewable primary energy EP (kWh/m^2) is lower or equal to the maximum value specified in the regulations (Table 6).
- The partitions and technical equipment of a building meet at least the thermal insulation requirements specified in Annex 2 of this Regulation (Table 7).

Table 6. Heat transfer coefficient of the external partitions required, from 2017 year (WT 2017) to 2021 year (WT 2021), for indoor spaces with $t_i \geq 16$ °C.

Partition	U_{2017} (W/m^{2}K)	U_{2021} (W/m^{2}K)
External wall	0.23	0.20
Roof	0.18	0.15
Floor on the ground	0.30	0.30
External door	1.50	1.30
External window (except roof)	1.10	0.90
External window (roof)	1.3	1.1

Table 7. Maximum partial values of the EP index for heating, ventilation, and domestic hot water (H + W); cooling (C); and lighting (L), in residential buildings from 1 January 2017 to 1 January 2021.

Building	Part	EP_{2017} (kWh/m^2)	EP_{2021} (kWh/m^2)
Single family	EP_{H+W}	95	70
	ΔEP_C	$10 \cdot A_{f,c}/A_f$	$5 \cdot A_{f,c}/A_f$
	ΔEP_L	0	0
Multifamily	EP_{H+W}	85	65
	ΔEP_C	$10 \cdot A_{f,c}/A_f$	$5 \cdot A_{f,c}/A_f$
	ΔEP_L	0	0

The maximum value of the indicator of the annual demand for nonrenewable primary energy EP is calculated according to the following formula:

$$EP = EP_{H+W} + \Delta EP_C + \Delta EP_L. \quad (68)$$

The calculation procedure to obtain EP is given in the Regulation of the Minister of Infrastructure and Development on the methodology for determining the energy performance of a building or part of a building and energy performance certificates [10]. It has been presented by several authors recently [99–101].

6. Results and Discussion

6.1. Solar Gains in the Single Family Building

In fact, to assess the impact of the solar irradiance modelling method on solar gains and heating demand, any of presented models can be used. However, as the reference point in all calculations the first model (TMY) was used because of the reasons presented in detail in Sections 1–3.

The calculated annual solar heat gains in locations I—V are shown in Figures 5 and 6 for Variants 1 and 2, respectively. The letter "C" means the cold half year (X—III). The letter "W" means the warm half year (IV—IX). The number "1" means TMY. Consecutive numbers from 2 to 16 refer to transposition models in the order shown in Section 4.

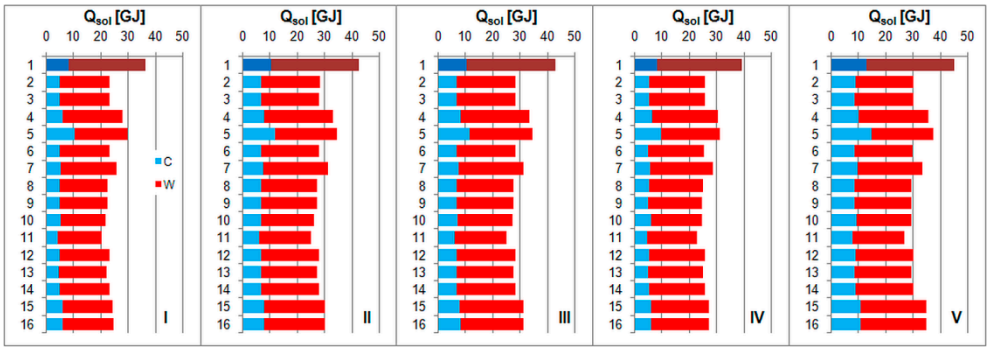

Figure 5. Total annual solar heat gains for Building 1, Variant 1.

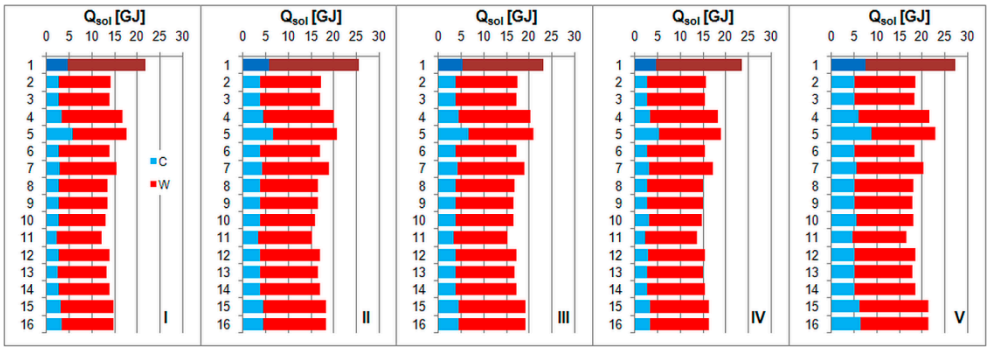

Figure 6. Total annual solar heat gains for Building 1, Variant 2.

For the TMYs, the calculated annual solar gains were from 36.5 GJ (location I) to 45.1 GJ (locationV); subsequently, for the other models, they ranged from 20.2 GJ (Model 11) to 29.7 GJ (Model 5), from 25.0 GJ (Model 11) to 34.5 GJ (Model 4), from 25.0 GJ (Model 11) to 34.6 GJ (Model 4), from 22.7 GJ (Model 11) to 31.4 GJ (Model 4), and from 26.8 GJ (Model 11) to 27.4 GJ (Model 4), in locations I–V, respectively. In all cases, solar heat gains calculated from the presented 15 models were significantly lower as compared with TMYs, with higher differences for the warm half year. The circumsolar (Model 4) and Skartveit and Olseth (Model 10) models provided the highest and lowest values of solar irradiance, respectively. Differences between the analysed models and values from TMYs were from 19% (Model 5) to 45% (Model 11), from 19% (Model 5) to 41% (Model 11), from 19% (Model 5) to 41% (Model 11), from 20% (Model 5) to 42% (Model 11), and from 17% (Model 5) to 41% (Model 11) in locations I–V, respectively.

The application of windows with lower solar energy transmittance and a reduction in their total area for Variant 2 resulted in a decrease in total annual solar gains by 40% on average. For TMYs, they varied from 21.8 GJ (location I) to 27.2 GJ (location V). In the case of other models, the values were from 12.2 GJ (Model 11) to 17.7 GJ (Model 5), from 15.2 GJ (Model 11) to 20.8 GJ (Model 5), from 15.3 GJ (Model 11) to 20.9 GJ (Model 5), from 13.8 GJ (Model 11) to 18.8 GJ (Model 5), and from 16.4 GJ (Model 11) to 22.7 GJ (Model 5) were noticed in locations I–V, respectively.

Differences between TMYs and other models were as follows: from 19% (Model 5) to 44% (Model 11), from 19% (Model 5) to 40% (Model 11), from 10% (Model 5) to 34% (Model 11), from 20% (Model 5) to 41% (Model 11), and from 17% (Model 5) to 40% (Model 11) in the same order. In both, the Variant 1 and 2 differences were very close.

In both the Variants 1 and 2, the highest values of solar gains were obtained by the circumsolar and Koronakis models, while the lowest were provided by the Ma and Iqbal model, and the Skartveit and Olseth model.

High values of solar irradiance calculated by the Koronakis model result from the method of calculating the R_d factor (Figure 7). In buildings, vertical walls dominate ($\beta = 90°$). In this case, $R_d = 0.67$ as compared with 0.5 for the Liu-Jordan and Badescu

models indicates about a 33% higher diffuse component of global solar irradiance calculated for the same area and weather conditions.

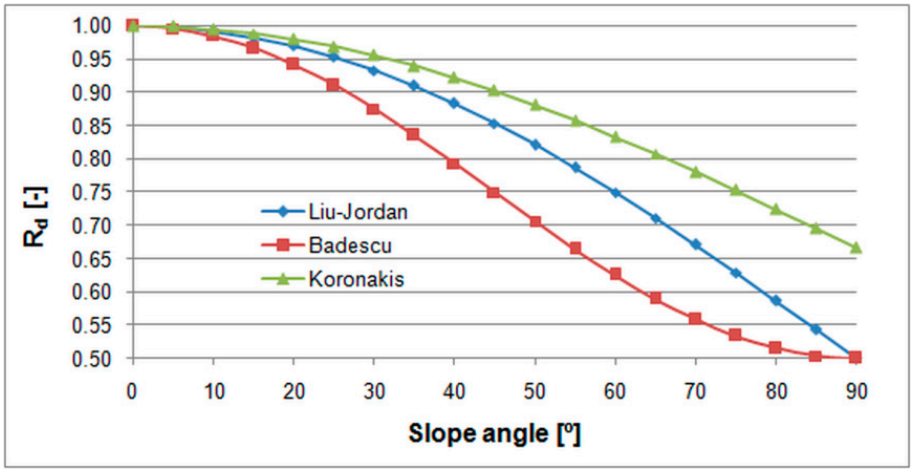

Figure 7. R_d factor for the Liu-Jordan, Badescu, and Koronakis models.

6.2. Solar Gains in the Multifamily Building

Solar heat gains in the multifamily building are shown in Figures 8 and 9 for the Variants 1 and 2, respectively.

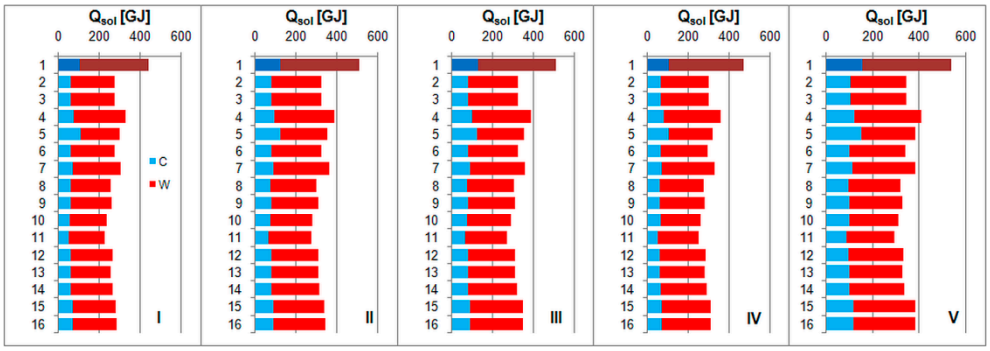

Figure 8. Total annual solar heat gains for Building 2, Variant 1.

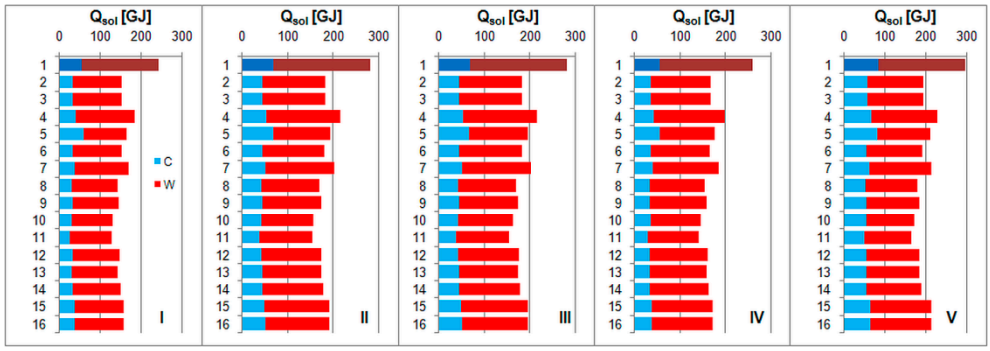

Figure 9. Total annual solar heat gains for Building 2, Variant 2.

For the TMYs, the calculated annual solar gains were from 440.9 GJ (location I) to 535.4 GJ (location V); subsequently, for the other models, they ranged from 227.6 GJ (Model 11) to 330.5 GJ (Model 4), from 273.5 GJ (Model 11) to 386.7 GJ (Model 4), from 271.8 GJ (Model 11) to 387.1 GJ (Model 4), from 249.0 GJ (Model 11) to 355.6 GJ (Model 4), and from 292.9 GJ (Model 11) to 410.2 GJ (Model 4), in locations I–V, respectively.

For the Variant 1, the differences in relation to TMYs were from 25% (Model 4) to 48% (Model 11), from 24% (Model 4) to 46% (Model 11), from 14% (Model 4) to 46% (Model 11), from 24% (Model 4) to 47% (Model 11), and from 23% (Model 5) to 45% (Model 11) in locations I–V, respectively.

Solar gains for the Variant 2, from TMYs, varied from 243.2 GJ (location I) to 296.5 GJ (location V). For the other models, the values were from 127.3 GJ (Model 11) to 183.4 GJ (Model 4), from 153.5 GJ (Model 11) to 215.4 GJ (Model 4), from 152.7 GJ (Model 11) to 215.6 GJ (Model 4), from 139.5 GJ (Model 11) to 197.7 GJ (Model 4), and from 164.8 GJ (Model 11) to 228.6 GJ (Model 4) were noticed in locations I–V, respectively. In relation to TMYs, the differences were as follows: 25% (Model 5) to 48% (Model 11), from 23% (Model 4) to 45% (Model 11), from 23% (Model 4) to 46% (Model 11), from 24% (Model 4) to 46% (Model 11), and from 23% (Model 5) to 44% (Model 11), in locations I–V, respectively.

In reference to values from TMYs, the application of the circumsolar model resulted in the greatest annual solar gains in most cases. These differences were, on average, 24% and 25%, for the first and second buildings, respectively. This is the consequence of a larger share of vertical walls in the total area of external partitions of the multifamily building (78.5%) than in the single-family building (62.5%). The highest differences were noticed in the case of the Skartveit and Olseth model and was47% and 46%, for the first and second buildings, respectively.

6.3. Annual Heating Energy Demand

The reference values in each location, calculated for the solar data from corresponding TMYs and for the Variant 1of the single-family building (Figure 10), were 57.3, 57.3, 60.2, 69.0 and 66.9 kWh/m^2 in locations I–V, respectively. In relation to the values from TMYs, the E_A index varied from −3% (Model 5) to 16% (Model 11), from −3% (Model 5) to 15% (Model 11), from −2% (Model 5) to 15% (Model 11), from −2% (Model 5) to 13% (Model 11), and from −1% (Model 5) to 18% (Model 11), respectively. For the Variant 2 (Figure 11), due to lower solar gains, the E_A indicator values were 63.2, 63.7, 68.2, 74.9, and 76.8 kWh/m^2, in locations I–V, respectively.

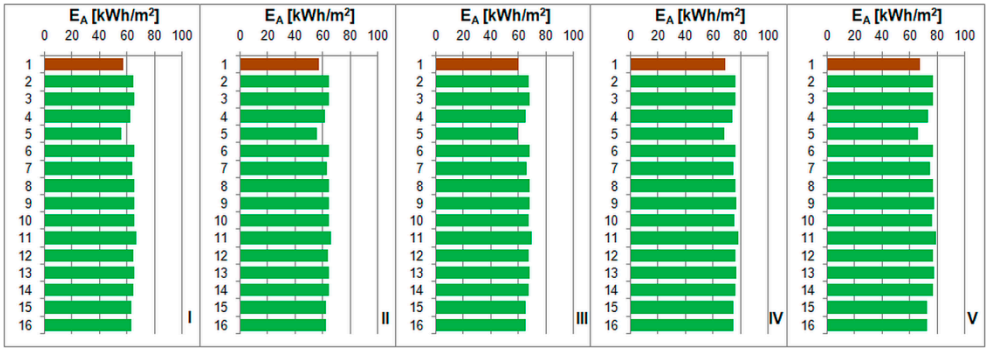

Figure 10. Annual heating energy consumption for Building 1, Variant 1.

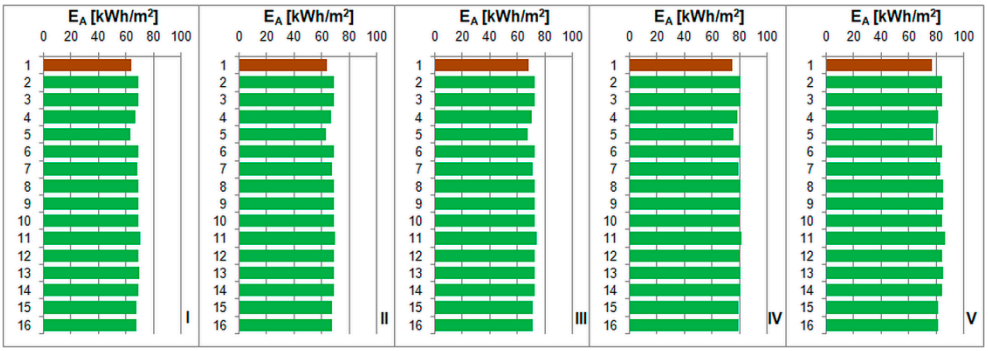

Figure 11. Annual heating energy consumption for Building 1, Variant 2.

In relation to TMYs, the situation was similar and the differences, in the same order, were from −1% (Model 5) to 11% (Model 11), from −1% (Model 5) to 9% (Model 11), from −2% (Model 5) to 8% (Model 11), from 0% (Model 5) to 9% (Model 11), and from 1% (Model 5) to 12% (Model 11),in locations I–V, respectively.

Application of the new EN ISO 52010 standard resulted in the E_A index greater from 4.9 kWh/m^2 (location II) to 5.4 kWh/m^2 (location III) and from 2.3 kWh/m^2 (location II) to 4.2 kWh/m^2 (location III) against the TMYs, for the Variants 1 and 2, respectively.

In the case of the second building (Figure 12), the situation was similar. The E_A indexes calculated for TMYs were31.2, 31.3, 33.2, 40.4 and 34.7 kWh/m^2 in locations I–V, respectively. In relation to TMYs, the value of that indicator for other models varied from −1% (Model 5) to 30% (Model 11), from −1% (Model 5) to 30% (Model 11), from 2% (Model 5) to 30% (Model 11), from 1% (Model 5) to 23% (Model 11), and from 5% (Model 5) to 35% (Model 11), in locations I–V, respectively.

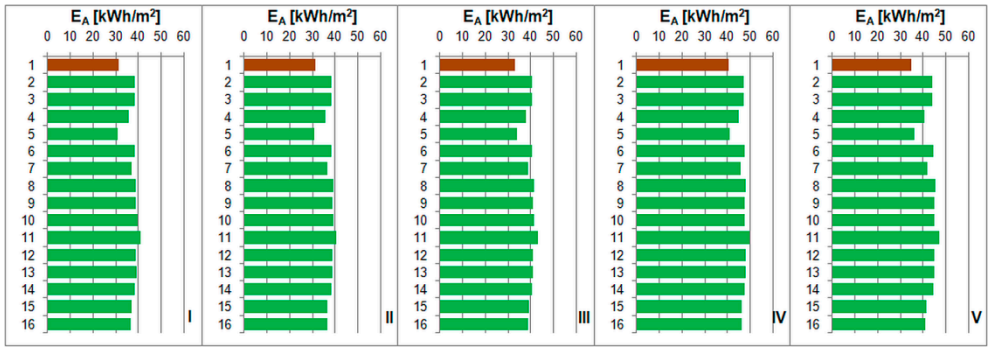

Figure 12. Annual heating energy consumption for Building 2, Variant 1.

For the Variant 2 (Figure 13), the differences were from 3% (Model 5) to 18% (Model 11), from 2% (Model 5) to 17% (Model 11), from 4% (Model 5) to 17% (Model 11), from 3% (Model 5) to 14% (Model 11), and from 6% (Model 5) to 20% (Model 11), respectively, in the same order. For both analysed variants of the multifamily building, application of the circumsolar model resulted in the calculated energy use for space heating value that was the closest value to the values using TMYs.

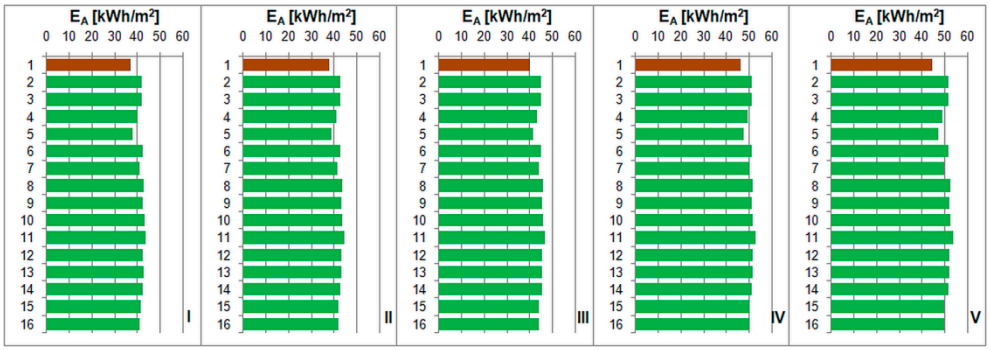

Figure 13. Annual heating energy consumption for Building 2, Variant 2.

The differences between TMYs and the EN ISO 52010 standard were from 5.1 kWh/m^2 (location IV) to 6.5 kWh/m^2 (location V) and from 3.8 kWh/m^2 (location IV) to 5.2 kWh/m^2 (location V), for the Variants 1 and 2, respectively.

Taking into consideration the aforementioned (in Section 5.3) E_A < 40 kWh/m^2 condition for this building, it can be seen that the adopted calculation method of solar irradiance has a significant impact on whether the building meets that criterion or not. Comparing the E_A indexes calculated from the TMYs and the new EN-ISO 52010 standard for the Variant 1 (Figure 12), it should be noted that they changed from 31.2, 31.3, 33.2, 40.4, and

34.7kWh/m^2 to 36.7, 36.4, 38.8, 46.0, and 41.1 kWh/m^2, in locations I–V, respectively. For the Variant 2, these values changed from 37.0, 37.9, 39.9, 46.1, and 44.4 kWh/m^2 to 41.1, 41.7, 44.0, 52.0, and 49.6 kWh/m^2, in locations I–V, respectively. This time, the new EN-ISO 52010-1 standard would result in the negative result in locations I, II, and III.

Theoretically, this example shows that, in the case of an energy efficient building, the choice of the solar irradiance calculation method results in an E_A index greater by several kWh/m^2. This is a significant change and may theoretically influence abuilding's energy performance.

The findings presented in Section 2 indicated that, for Polish climatic global solar irradiance on a tilted plane, the best results were achieved by the Koronakis (Model 5), Hay (Model 8), Reindl (Model 12), Gueymard (Model 13), Muneer (Model 14), and Perez (Model 15) models [19,20]. The Koronakis and circumsolar models should be excluded because of the significant solar gains they provided. For the other models, comparable results were noticed. The E_A index was higher on average by 11% and 20% (Hay), 13% and 17% (Reindl), 11% and 19% (Gueymard), 10% and 19% (Muneer), and finally 7% and 14% (Perez), for the first and second building, respectively.

6.4. Energy Performance Indicators

Taking into consideration the assumptions presented in the previous sections, in the single-family building, the primary energy for domestic hot water preparation was the same in all locations and was 11.3 kWh/m^2. Hence, the values of the EP_{H+W} indicator were calculated, as shown in Figures 14 and 15, for the Variants 1 and 2, respectively. In the first case, the reference value of EP_{H+W} for current TMYs was from 35.6 kWh/m^2 (location I) to 39.3 kWh/m^2 (location IV). Similarly, as in the previous section, the lowest and the greatest values of EP_{H+W} were obtained for Models5 and 11, respectively, and were from 35.0 to 38.6, from 35.0 to 38.3, from 36.2 to 39.5, from 39.0 to 42.2, and from 38.4 to 42.5 kWh/m^2, in locations I–V, respectively. The differences between Model 16 (the new standard) and TMYs were from 1.5 (location II) to 1.7 kWh/m^2 (location III) with a mean of 1.6 kWh/m^2.

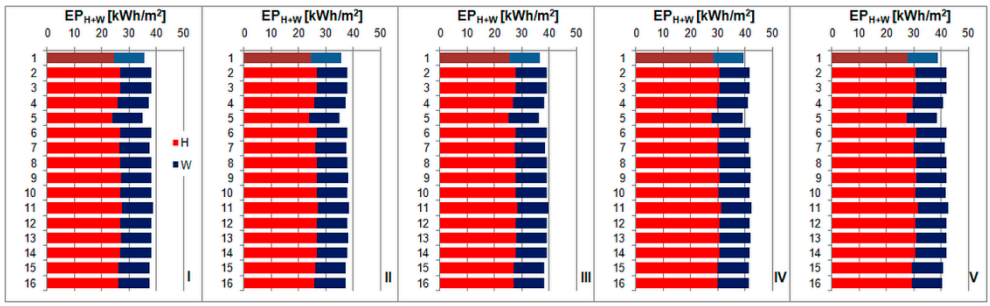

Figure 14. EP_{H+W} indicator for Building 1, Variant 1.

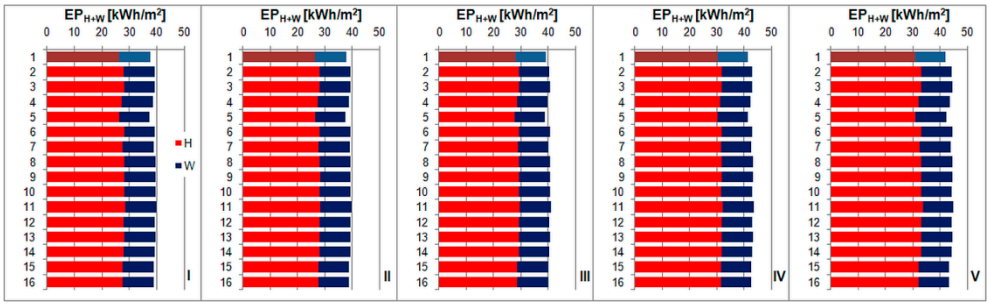

Figure 15. EP_{H+W} indicator for Building 1, Variant 2.

For the Variant 2, the reference EP_{H+W} was from 37.5 kWh/m^2 (location I) to 41.8 kWh/m^2 (location V). The calculations performed for the new standard resulted in values greater by 0.8 (location III) to 1.3 kWh/m^2 (location IV) with a mean of 1.2 kWh/m^2.

In Building 2, due to its different character, the primary energy for domestic hot water was greater, i.e., 27.0 kWh/m^2. For the Variant 1 (Figure 16), the EP_{H+W} was from 55.3 kWh/m^2 (location I) to 63.5 kWh/m^2 (location IV) and from 60.2 (location II) to 68.7 kWh/m^2 (location IV) for the TMYs and new standard, respectively. For the Variant 2 (Figure 17), the EP_{H+W} was from 60.5 kWh/m^2 (location I) to 68.7 kWh/m^2 (location IV) and from 64.2 (location I) to 72.4 kWh/m^2 (location V) for the TMYs and new standard, respectively. Consequently, the resulting difference between them was from 4.6 to 5.9 kWh/m^2 (mean 5.1 kWh/m^2) and from 3.4 to 4.7 kWh/m^2 (mean 3.9 kWh/m^2) for the Variants 1 and 2, respectively.

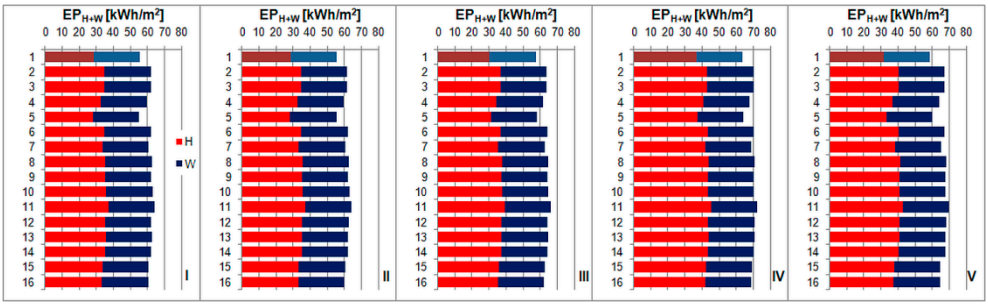

Figure 16. EP_{H+W} indicator for Building 2, Variant 1.

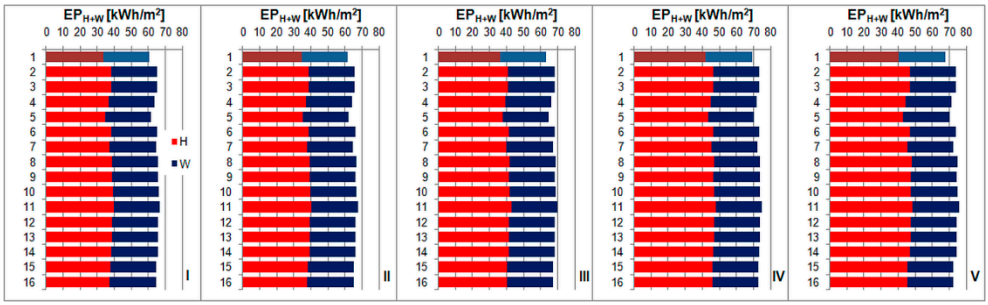

Figure 17. EP_{H+W} indicator for Building 2, Variant 2.

7. Conclusions

In this study, global solar irradiance on sloped surfaces in five locations in Poland were calculated using hourly horizontal irradiance from Polish typical meteorological years (TMYs) as input data for 15 transposition models (isotropic, pseudo-isotropic, and anisotropic). Then, solar gains, heating demands, and energy performance indicators for two typical residential buildings were calculated and compared with values calculated on the bases of the data provided in TMYs for sloped surfaces at typical slope angles.

The highest differences in annual heating demands were observed for the Skartveit and Olseth model, i.e., 13% and 24% on average for the first and second building, respectively. The lowest disagreement was obtained for the circumsolar model, i.e., −2% and 3%, for the first and second building, respectively. The application of models recommended in Polish conditions in other studies have resulted in maximum differences of 10% and 20% (Hay), 10% and 19% (Reindl), 11% and 19% (Gueymard), 10% and 18% (Muneer), and 7% and 14% (Perez).

The presented results showed that the model used in the calculations of irradiance on sloped surfaces in Polish TMYs significantly overestimated computed values, especially for vertical walls. Hence, it should not be used for building energy performance modelling. The same conclusion can be applied to the circumsolar and Koronakis models.

The new calculation method of EN ISO 52010-1 introduced the anisotropic Perez model. In the first building, the value of EP_{H+W} calculated by that model differed, on average, from that by TMYs by 1.6 and 1.2 kWh/m^2, for the Variants 1 and 2, respectively. Similarly, in Building 2, it was 5.1and 3.9 kWh/m^2. It indicates that the calculation of solar

irradiance according to the EN ISO 52010-1 standard results in a noticeable change of EP_{H+W} indicator in relation to that provided in Polish TMYs, influencing the energy rating of a building. This is a very important outcome since these discrepancies occurred without any physical modernisation works and resulted only from changing the calculation method.

The results presented on aggregated monthly (heating needs) and an annual (energy performance indicators) level confirm that a more detailed analysis is also necessary in an hourly step, and therefore possible differences in an instantaneous thermal (heating and cooling) power could be obtained and the impact of the applied calculation method on thermal performance of building, thermal comfort, or overheating risk could be analysed.

The calculation methods presented in the study can also be applied in any location for which at least global hourly solar irradiance data are available.

Supplementary Materials: The following are available online at https://www.mdpi.com/article/10.3390/en14144371/s1, Spreadsheet S1: Typical meteorological years for Koszalin, Poznań, Kielce, Białystok, and Zakopane in hourly format.

Funding: This research received no external funding.

Institutional Review Board Statement: Not applicable.

Informed Consent Statement: Not applicable.

Data Availability Statement: Not applicable.

Conflicts of Interest: The author declares no conflict of interest.

Nomenclature

A_c —projected area of an envelope element, m^2
A_{sol} —effective collecting area of an envelope element, m^2
A_f —total conditioned (heated and/or cooled) floor area, m^2
$A_{f,c}$ —total cooled floor area, m^2
A_c —projected area of an envelope element, m^2
A_{sol} —effective collecting area of an envelope element, m^2
B —Earth orbit deviation, °
C_m —internal thermal capacity of the considered building (or zone), J/K
E_A —annual heating energy demand per unit floor area of a building, kWh/m^2
EP_{H+W} —partial maximum value of the EP index for heating, ventilation and domestic hot water, kWh/m^2
EP —index of the annual demand for nonrenewable primary energy, kWh/m^2
EU —usable energy indicator, kWh/m^2
F_F —frame and divider area fraction of the glazed element
F_{sky} —view factor between the element and the sky
$F_{sh,ob}$ —shading reduction factor for external obstacles
$F_{sh,gl}$ —shading reduction factor for movable shading provisions
F_1 —circumsolar brightness coefficient
F_2 —horizontal brightness coefficient
$G_{sol,c}$ —solar constant, 1370 W/m^2
H —solar irradiation, kWh/m^2
H_{tr} —heat transfer coefficient by transmission, W/K
H_{ve} —heat transfer coefficient by ventilation, W/K
$I_{b,h}$ —direct (beam) solar irradiance on a horizontal surface, W/m^2
$I_{b,s}$ —direct (beam) solar irradiance on a sloped surface, W/m^2
$I_{d,h}$ —diffuse solar irradiance on a horizontal surface, W/m^2
$I_{d,s}$ —diffuse solar irradiance on a sloped surface, W/m^2
I_{ext} —extra-terrestrial irradiance, W/m^2
$I_{ext,h}$ —extra-terrestrial irradiance on a horizontal surface, W/m^2
$I_{g,h}$ —global solar irradiance on a horizontal surface, W/m^2
$I_{g,s}$ —global solar irradiance on a sloped surface, W/m^2
$I_{r,s}$ —solar irradiance due to ground reflection on a sloped surface, W/m^2
I_{tot} —calculated total solar irradiance, W/m^2
R_b —beam (direct) transposition factor
Q_{sol} —solar heat gain, J
R_d —diffuse transposition factor
R_r —reflected transposition factor

R_{se} —external surface heat resistance of an element, $m^2 \cdot K/W$
T_{shift} —time shift, h
TZ —time zone, h
U —thermal transmittance, $W/(m^2 \cdot K)$
U_c — thermal transmittance of an envelope element of the area Ac, $W/(m^2 \cdot K)$
f —brightness coefficient (Perez model)
g_{gl} —monthly mean effective total solar energy transmittance
i —month number
$h_{r,e}$ —external radiative heat transfer coefficient, $W/(m^2 \cdot K)$
k_H —anisotropy index (Hay model)
k_R —modulating factor (Reindl model)
k_T —clearness index of the atmosphere
m —air mass
n_{day} —day of the year
n_{hour} —actual (clock) hour for the location (counting number of the hour in the day)
t_{eq} —equation of time, min
t_s —solar time, h
t_i —internal air temperature, °C
Δ —sky brightness parameter
ΔEP_C —partial value of the EP index for cooling, kWh/m^2
ΔEP_L —partial value of the EP index for lighting, kWh/m^2
$\Delta\theta_{sky}$ — average difference between the external air temperature and the apparent sky temperature, K
$\Delta\tau_m$ —length of the m-th month, s
Φ_r —heat flow due to thermal radiation to the sky, W
Φ_{sol} —heat flow by solar gains through a building element, W
α_{op} —absorption coefficient for solar radiation of the opaque element
α_{sol} —solar altitude angle, °
β —slope angle of inclined surface, °
γ —azimuth angle, °
δ —solar declination, °
ε —clearness parameter (Perez model)
θ —angle of incidence of beam irradiance, °
θ_z —zenith angle, °
λ_w —longitude of a weather station, °
ρ —solar reflectivity of the ground and building's surroundings
φ_w —latitude of a weather station, °
ω —solar hour angle, °

References

1. *Energy Consumption in Households in 2018*; Central Statistical Office: Warsaw, Poland, 2019. Available online: https://stat.gov.pl/en/topics/environment-energy/energy/energy-consumption-in-households-in-2018,2,5.html (accessed on 14 April 2021).
2. Kozik, R.; Karasińska-Jaśkowiec, I. Green public procurement-legal base and instruments supporting sustainable development in the construction industry in Poland. *E3S Web Conf.* **2016**, *10*, 00044. [CrossRef]
3. Ramczyk, M. Legal bases and economic conditions of applying renewable energy resources in construction industry. *MATEC Web Conf.* **2018**, *174*, 04004. [CrossRef]
4. European Parliament and Council. Directive 2010/31/EU of the European Parliament and of the Council of 19 May 2010 on the energy performance of buildings (recast). *Off. J. Eur. Union* **2010**, 13–35. Available online: http://eur-lex.europa.eu/LexUriServ/LexUriServ.do?uri=OJ:L:2010:153:0013:0035:EN:PDF (accessed on 14 April 2021).
5. Gonzalez Caceres, A.; Diaz, M. Usability of the EPC tools for the profitability calculation of a retrofitting in a residential building. *Sustainability* **2018**, *10*, 3159. [CrossRef]
6. Firląg, S. How to Meet the Minimum Energy Performance Requirements of Technical Conditions in Year 2021? *Procedia Eng.* **2015**, *111*, 202–208. [CrossRef]
7. Szul, T. The consumption of final energy for heating educational facilities located in rural areas. *J. Res. Appl. Agric. Eng.* **2017**, *62*, 171–175. Available online: https://www.pimr.eu/wp-content/uploads/2019/05/2017_1_TS.pdf (accessed on 14 April 2021).
8. Fedorczak-Cisak, M.; Kowalska-Koczwara, A.; Kozak, E.; Pachla, F.; Szuminski, J.; Tatara, T. Energy and Cost Analysis of Adapting a New Building to the Standard of the NZEB. *IOP Conf. Ser. Mater. Sci. Eng.* **2019**, *471*, 112076. [CrossRef]
9. Ordinance of the Minister of Infrastructure and Development of 17 July 2015 Amending the Regulation on Technical Conditions to Be Met by Buildings and Their Location. Available online: http://isap.sejm.gov.pl/isap.nsf/download.xsp/WDU20190001065/O/D20191065.pdf (accessed on 14 April 2021). (In Polish)
10. Regulation of the Minister of Infrastructure and Development of 27 February 2015 on the Methodology to Determine the Energy Performance of a Building or Part of a Building, and Energy Performance Certificates. Available online: http://isap.sejm.gov.pl/isap.nsf/DocDetails.xsp?id=WDU20150000376 (accessed on 14 April 2021). (In Polish)
11. de Ayala, A.; Galarraga, I.; Spadaro, J.V. The price of energy efficiency in the Spanish housing market. *Energy Policy* **2016**, *94*, 16–24. [CrossRef]
12. Fokaides, P.A.; Polycarpou, K.; Kalogirou, S. The impact of the implementation of the European Energy Performance of Buildings Directive on the European building stock: The case of the Cyprus Land Development Corporation. *Energy Policy* **2017**, *11*, 1–8. [CrossRef]

13. Typical Meteorological Years. The Ministry of Infrastructure and Development. Available online: https://archiwum.miir.gov.pl/strony/zadania/budownictwo/charakterystyka-energetyczna-budynkow/dane-do-obliczen-energetycznych-budynkow-1/ (accessed on 14 April 2021).
14. Narowski, P. Methods for determining typical meteorological years TMY2, WYEC2 and according to EN ISO 15927-4. *Dist. Heat. Heat. Vent.* **2014**, *45*, 479–485. Available online: https://sigma-not.pl/publikacja-88288-metody-wyznaczania-typowych-lat-meteorologicznych-tmy2,-wyec2-oraz-wed\T1\lug-normy-en-iso-15927-4-cieplownictwo-ogrzewnictwo-wentylacja-2014-12.html (accessed on 14 April 2021). (In Polish).
15. EN ISO 52010-1:2017. *Energy Performance of Buildings-External Climatic Conditions—Part 1: Conversion of Climatic Data for Energy Calculations*; ISO: Geneva, Switzerland, 2017.
16. Horvat, I.; Dović, D. Dynamic modeling approach for determining buildings technical system energy performance. *Energy Convers. Manag.* **2016**, *125*, 154–165. [CrossRef]
17. Raptis, P.I.; Kazadzis, S.; Psiloglou, B.; Kouremeti, N.; Kosmopoulos, P.; Kazantzidis, A. Measurements and model simulations of solar radiation at tilted planes, towards the maximization of energy capture. *Energy* **2017**, *130*, 570–580. [CrossRef]
18. Khalil, S.A.; Shaffie, A.M. A comparative study of total, direct and diffuse solar irradiance by using different models on horizontal and inclined surfaces for Cairo, Egypt. *Renew. Sustain. Energy Rev.* **2013**, *27*, 853–863. [CrossRef]
19. Chwieduk, D.A. Recommendation on modelling of solar energy incident on a building envelope. *Renew. Energy* **2009**, *34*, 736–741. [CrossRef]
20. Włodarczyk, D.; Nowak, H. Statistical analysis of solar radiation models onto inclined planes for climatic conditions of Lower Silesia in Poland. *Arch. Civ. Mech. Eng.* **2009**, *9*, 127–144. [CrossRef]
21. Kulesza, K. Comparison of typical meteorological year and multi-year time series of solar conditions for Belsk, central Poland. *Renew. Energy* **2017**, *113*, 1135–1140. [CrossRef]
22. Frydrychowicz-Jastrzębska, G.; Bugała, A. Modeling the Distribution of Solar Radiation on a Two-Axis Tracking Plane for Photovoltaic Conversion. *Energies* **2015**, *8*, 1025–1041. [CrossRef]
23. Chwieduk, D.; Chwieduk, M. Determination of the Energy Performance of a Solar Low Energy House with Regard to Aspects of Energy Efficiency and Smartness of the House. *Energies* **2020**, *13*, 3232. [CrossRef]
24. Trząski, A.; Panek, A.; Rucińska, J. Impact of windows parameters on the thermal performance of a multi-family building. *Tech. Trans. Civ. Eng.* **2014**, *3-B*, 473–480. Available online: https://repozytorium.biblos.pk.edu.pl/resources/30509 (accessed on 14 April 2021).
25. Ferdyn-Grygierek, J.; Grygierek, K. Optimization of window size design for detached house using TRNSYS simulations and genetic algorithm. *Archit. Civ. Eng. Environ.* **2017**, *10*, 133. Available online: http://acee-journal.pl/1,7,45,Issues.html (accessed on 14 April 2021). [CrossRef]
26. Kwiatkowski, J.; Rucińska, J.; Panek, A. Analysis of different shading strategies on energy demand and operating cost of office building. In Proceedings of the World Sustainable Building Conference SB14, Barcelona, Spain, 28–30 October 2014; pp. 512–521. Available online: http://wsb14barcelona.org/programme/pdf_poster/P-101.pdf (accessed on 14 April 2021).
27. Błaszkiewicz, Z.; Kneblewski, P. The identification of selected window energy parameters in winter and summer periods in the Greater Poland region. *J. Res. Appl. Agric. Engngy* **2018**, *63*, 8–12. Available online: https://www.pimr.eu/wp-content/uploads/2019/05/2018_1_BK.pdf (accessed on 14 April 2021).
28. Chwieduk, D.A. Some aspects of modelling the energy balance of a room in regard to the impact of solar energy. *Sol. Energy* **2008**, *82*, 870–884. [CrossRef]
29. Chwieduk, D. Impact of solar energy on the energy balance of attic rooms in high latitude countries. *Appl. Therm. Eng.* **2018**, *136*, 548–559. [CrossRef]
30. Shaeri, J.; Habibi, A.; Yaghoubi, M.; Chokhachian, A. The Optimum Window-to-Wall Ratio in Office Buildings for Hot-Humid, Hot-Dry, and Cold Climates in Iran. *Environments* **2019**, *6*, 45. [CrossRef]
31. Premrov, M.; Žigart, M.; Žegarac Leskovar, V. Influence of the building shape on the energy performance of timber-glass buildings located in warm climatic regions. *Energy* **2018**, *149*, 496–504. [CrossRef]
32. Michalak, P. Modelling of global solar irradiance on sloped surfaces in climatic conditions of Kraków. *New Trends Prod. Eng.* **2019**, *2*, 505–514. [CrossRef]
33. Prada, A.; Pernigotto, G.; Baggio, P.; Gasparella, A.; Mahdavi, A. Effect of Solar Radiation Model on the Predicted Energy Performance of Buildings. International High Performance Buildings Conference 2014. p. 130. Available online: http://docs.lib.purdue.edu/ihpbc/130 (accessed on 1 July 2021).
34. Pernigotto, G.; Prada, A.; Baggio, P.; Gasparella, A.; Mahdavi, A. Solar Irradiance Modelling and Uncertainty on Building Hourly Profiles of Heating and Cooling Energy Needs. In Proceedings of the International High Performance Buildings Conference, West Lafayette, IN, USA, 11–14 July 2016; p. 191. Available online: http://docs.lib.purdue.edu/ihpbc/191 (accessed on 6 July 2021).
35. Błażejczyk, K. Natural and human environment of Poland. A geographical overview. In *Climate and Bioclimate of Poland*; Degórski, M., Ed.; Polish Academy of Sciences Institute of Geography and Spatial Organization, Polish Geographical Society: Warsaw, Poland, 2006; pp. 31–48. Available online: http://rcin.org.pl/Content/36223/WA51_45533_r2006_Natural-human-enviro.pdf (accessed on 14 April 2021).
36. Igliński, B.; Kujawski, W.; Buczkowski, R.; Cichosz, M. Renewable energy in the Kujawsko-Pomorskie Voivodeship (Poland). *Renew. Sustain. Energy Rev.* **2010**, *14*, 1336–1341. [CrossRef]

37. Igliński, B.; Buczkowski, R.; Cichosz, M.; Piechota, G.; Kujawski, W.; Plaskacz, M. Renewable energy production in the Zachodniopomorskie Voivodeship (Poland). *Renew. Sustain. Energy Rev.* **2013**, *27*, 768–777. [CrossRef]
38. Igliński, B.; Iglińska, A.; Cichosz, M.; Kujawski, W.; Buczkowski, R. Renewable energy production in the Łódzkie Voivodeship. The PEST analysis of the RES in the voivodeship and in Poland. *Renew. Sustain. Energy Rev.* **2016**, *58*, 737–750. [CrossRef]
39. Kleniewska, M.; Chojnicki, B.H.; Acosta, M. Long-term total solar radiation variability at the Polish Baltic coast in Kołobrzeg within the period 1964–2013. *Meteorol. Hydrol. Water Manag.* **2016**, *4*, 35–40. [CrossRef]
40. Prvulovic, S.; Tolmac, D.; Matic, M.; Radovanovic, L.; Lambic, M. Some aspects of the use of solar energy in Serbia. *Energy Sources Part B Econ. Plan. Policy* **2018**, *13*, 237–245. [CrossRef]
41. Igliński, B.; Cichosz, M.; Kujawski, W.; Plaskacz-Dziuba, M.; Buczkowski, R. Helioenergy in Poland—Current state, surveys and prospects. *Renew. Sustain. Energy Rev.* **2016**, *58*, 862–870. [CrossRef]
42. Magiera, J.; Pater, S. Bivalent heating installation with a heat pump and solar collectors for a residential building. *Environ. Prot. Eng.* **2012**, *38*, 127–140. [CrossRef]
43. Pater, S. Field measurements and energy performance analysis of renewable energy source devices in a heating and cooling system in a residential building in southern Poland. *Energy Build.* **2019**, *199*, 115–125. [CrossRef]
44. Wierciński, Z.; Skotnicka-Siepsiak, A. Energy and exergy flow balances for traditional and passive detached houses. *Bull. Pol. Acad. Sci. Tech. Sci.* **2012**, *15*, 15–33. Available online: http://www.uwm.edu.pl/wnt/technicalsc/tech_15_1/B02.pdf (accessed on 14 April 2021).
45. Hurnik, M.; Specjał, A.; Popiołek, Z.; Kierat, W. Assessment of single-family house thermal renovation based on comprehensive on-site diagnostics. *Energy Build.* **2018**, *58*, 162–171. [CrossRef]
46. Typical Meteorological Years and Statistical Climatic Data for the Area of Poland for Energy Calculations of Buildings. Ministry of Economic Development, Labour and Technology. Available online: https://dane.gov.pl/pl/dataset/797,typowe-lata-meteorologiczne-i-statystyczne-dane-klimatyczne-dla-obszaru-polski-do-obliczen-energetycznych-budynkow (accessed on 1 July 2021).
47. Narowski, P. Climatic data for energy calculations of buildings. *Energ. Budynek* **2008**, *9*, 18–24. Available online: https://www.buildup.eu/pl/practices/publications/dane-klimatyczne-do-obliczen-energetycznych-budynkow (accessed on 1 July 2021). (In Polish).
48. Narowski, P. Energy calculations for buildings. Typical meteorological years and statistical climatic data for the area of Poland. *Rynek Instal.* **2008**, *16*, 52–57. Available online: https://www.buildup.eu/en/node/5553 (accessed on 1 July 2021). (In Polish).
49. Narowski, P.; Heim, D. Climatic data for modelling of hygrothermal processes in building elements. *Build. Phys. Theory Pract.* **2008**, *3*, 85–91. Available online: http://yadda.icm.edu.pl/baztech/element/bwmeta1.element.baztech-article-LOD6-0006-0015 (accessed on 1 July 2021). (In Polish).
50. Narowski, P.; Janicki, M.; Heim, D. Weather year for energy calculation (WYEC2) for optimisation of double skin façade. *Build. Phys. Theory Pract.* **2011**, *6*, 67–76. Available online: http://yadda.icm.edu.pl/yadda/element/bwmeta1.element.baztech-bd2ed253-5230-44f2-a857-824bdb7684a9 (accessed on 24 June 2021). (In Polish).
51. Lundström, L.; Akander, J.; Zambrano, J. Development of a Space Heating Model Suitable for the Automated Model Generation of Existing Multifamily Buildings—A Case Study in Nordic Climate. *Energies* **2019**, *12*, 485. [CrossRef]
52. Demain, C.; Journée, M.; Bertrand, C. Evaluation of different models to estimate the global solar radiation on inclined surfaces. *Renew. Energy* **2013**, *50*, 710–721. [CrossRef]
53. de Simón-Martín, M.; Alonso-Tristán, C.; Díez-Mediavilla, M. Diffuse solar irradiance estimation on building's façades: Review, classification and benchmarking of 30 models under all sky conditions. *Renew. Sustain. Energy Rev.* **2017**, *77*, 783–802. [CrossRef]
54. Danandeh, M.A.; Mousavi, G.S.M. Solar irradiance estimation models and optimum tilt angle approaches: A comparative study. *Renew. Sustain. Energy Rev.* **2018**, *92*, 319–330. [CrossRef]
55. Khalil, S.A.; Shaffie, A.M. Evaluation of transposition models of solar irradiance over Egypt. *Renew. Sustain. Energy Rev.* **2016**, *66*, 105–119. [CrossRef]
56. Yang, D. Solar radiation on inclined surfaces: Corrections and benchmarks. *Sol. Energy* **2016**, *136*, 288–302. [CrossRef]
57. Gul, M.; Kotak, Y.; Muneer, T.; Ivanova, S. Enhancement of Albedo for Solar Energy Gain with Particular Emphasis on Overcast Skies. *Energies* **2018**, *11*, 2881. [CrossRef]
58. Kondratyev, K.J.; Manolova, M.P. The Radiation Balance of Slopes. *Sol. Energy* **1960**, *4*, 14–19. [CrossRef]
59. Liu, B.Y.H.; Jordan, R.C. A rational procedure for predicting the long-term average performance of flat-plate solar-energy collectors: With design data for the U.S., its outlying possessions and Canada. *Sol. Energy* **1963**, *7*, 53–74. [CrossRef]
60. Badescu, V. 3D isotropic approximation for solar diffuse irradiance on tilted surfaces. *Renew. Energy* **2002**, *26*, 221–233. [CrossRef]
61. Iqbal, M. *An Introduction to Solar Radiation*; Academic Press: Cambridge, MA, USA, 1983.
62. Koronakis, P.S. On the choice of the angle of tilt for south facing solar collectors in the Athens basin area. *Sol. Energy* **1986**, *36*, 217–225. [CrossRef]
63. Bugler, J.W. The determination of hourly insolation on an inclined plane using a diffuse irradiance model based on hourly measured global horizontal insolation. *Sol. Energy* **1977**, *19*, 477–491. [CrossRef]
64. Klucher, T. Evaluation of models to predict insolation on tilted surfaces. *Sol. Energy* **1979**, *23*, 111–114. [CrossRef]
65. Hay, J.E. Calculating solar radiation for inclined surfaces: Practical approaches. *Renew. Energy* **1993**, *3*, 373–380. [CrossRef]

66. Willmott, C.J. On the climatic optimization of the tilt and azimuth of flatplate solar collectors. *Sol. Energy* **1982**, *28*, 205–216. [CrossRef]
67. Ma, C.; Iqbal, M. Statistical comparison of models for estimating solar radiation on inclined surfaces. *Sol. Energy* **1983**, *31*, 313–317. [CrossRef]
68. Skartveit, A.; Olseth, J.A. Modelling slope irradiance at high latitudes. *Sol. Energy* **1986**, *36*, 333–344. [CrossRef]
69. Reindl, D.; Beckman, W.; Duffie, J. Evaluation of hourly tilted surface radiation models. *Sol. Energy* **1990**, *45*, 9–17. [CrossRef]
70. Gueymard, C. An anisotropic solar irradiance model for tilted surfaces and its comparison with selected engineering algorithms. *Sol. Energy* **1987**, *38*, 367–386. [CrossRef]
71. Muneer, T. Solar radiation model for Europe. *Build. Serv. Eng. Res. Technol.* **1990**, *11*, 153–163. [CrossRef]
72. Perez, R.; Stewart, R.; Seals, R.; Guertin, T. *The Development and Verification of the Perez Diffuse Radiation Model. Atmospheric Sciences Research Center SUNY at Albany*; US Department of Energy Office of Scientific and Technical Information: Oak Ridge, TN, USA, 1988. Available online: https://www.osti.gov/biblio/7024029 (accessed on 14 April 2021).
73. PN-EN 12831. *Energy Performance of Buildings-Method for Calculation of the Design Heat Load-Part 1: Space Heating Load*; ISO: Geneva, Switzerland, 2017.
74. Nowak, S. Management of Heat Energy Consumption in Poland for The Purpose Of Buildings' Heating and Preparation of Useable, Hot Water. *Ann. Univ. Apulensis Ser. Oeconomica* **2009**, *11*, 895–901. Available online: http://www.oeconomica.uab.ro/upload/lucrari/1120092/33.pdf (accessed on 14 April 2021).
75. Dylewski, R.; Adamczyk, J. The environmental impacts of thermal insulation of buildings including the categories of damage: A Polish case study. *J. Clean. Prod.* **2016**, *137*, 878–887. [CrossRef]
76. Solar Resource Maps of Poland; Global Horizontal Irradiation. 2019 The World Bank, Source: Global Solar Atlas 2.0, Solar Resource Data. Available online: https://solargis.com/maps-and-gis-data/download/poland (accessed on 14 April 2021).
77. EnergyPlus Weather Database. Available online: https://energyplus.net/weather (accessed on 14 April 2021).
78. *Polish Building Typology—Scientific Report Composed within The Framework of the IEE Funded TABULA Project 2011/TEM/R/091763*; Narodowa Agencja Poszanowania Energii SA: Warsaw, Poland, 2012; Available online: http://episcope.eu/fileadmin/tabula/public/docs/scientific/PL_TABULA_ScientificReport_NAPE.pdf (accessed on 14 April 2021).
79. Beagon, P.; Boland, F.; Saffari, M. Closing the gap between simulation and measured energy use in home archetypes. *Energy Build.* **2020**, *224*, 110244. [CrossRef]
80. Jędrzejuk, H.; Dybiński, O. The influence of a heating system control program and thermal mass of external walls on the internal comfort in the Polish climate. *Energy Procedia* **2015**, *78*, 1087–1092. [CrossRef]
81. Firląg, S.; Piasecki, M. NZEB Renovation Definition in a Heating Dominated Climate: Case Study of Poland. *Appl. Sci.* **2018**, *8*, 1605. [CrossRef]
82. Życzyńska, A.; Cholewa, T. The modifications to the requirements on energy savings and thermal insulation of buildings in Poland in the years 1974–2021. *Bud. Archit.* **2015**, *14*, 145–154. Available online: http://wbia.pollub.pl/files/85/attachment/vol14%281%29/145-154.pdf (accessed on 14 April 2021). [CrossRef]
83. Krzeszowski, Ś. Evaluation of the usefulness of selected computer programs in the context of educating students of the environmental engineering. *Chem. Didact. Ecol. Metrol.* **2015**, *20*, 31–37. [CrossRef]
84. Mindykowski, D. Optimization of Heating and Cooling System for a Passive House Equipped with Heat Pump and Heat storage. Master's Thesis, Norwegian University of Science and Technology, Trondheim, Norway, 2016. Available online: https://ntnuopen.ntnu.no/ntnu-xmlui/handle/11250/2405175 (accessed on 14 April 2021).
85. Firląg, S. Cost-Optimal Plus Energy Building in a Cold Climate. *Energies* **2019**, *12*, 3841. [CrossRef]
86. Wojdyga, K.; Chorzelski, M. Chances for Polish district heating systems. *Energy Procedia* **2017**, *116*, 106–118. [CrossRef]
87. Drozd, W.; Kowalik, M. Analysis of renewable energy use in single-family housing. *Open Eng.* **2019**, *9*, 269–281. [CrossRef]
88. Starakiewicz, A. Coverage of energy for the preparation of hot tap water by installing solar collectors in a single-family building. *E3S Web Conf.* **2018**, *49*, 00106. [CrossRef]
89. Dudkiewicz, E.; Fidorów-Kaprawy, N. Hybrid Domestic Hot Water System Performance in Industrial Hall. *Resources* **2020**, *9*, 65. [CrossRef]
90. Oliveira Panão, M.J.N.; Santos, C.A.P.; Mateus, N.M.; Carrilho da Graca, G. Validation of a lumped RC model for thermal simulation of a double skin natural and mechanical ventilated test cell. *Energy Build.* **2016**, *121*, 92–103. [CrossRef]
91. *EN ISO 13790: Energy Performance of Buildings—Calculation of Energy Use for Space Heating and Cooling*; ISO: Geneva, Switzerland, 2008.
92. Kowalski, P.; Szałański, P. Computational and the real energy performance of a single-family residential building in Poland—An attempt to compare: A case study. *E3S Web Conf.* **2017**, *17*, 00045. [CrossRef]
93. Jędrzejuk, H.; Dojnikowska, J. On some aspects of modernisation of a wooden house with special cultural value. *E3S Web Conf.* **2018**, *49*, 00050. [CrossRef]
94. Firląg, S.; Zawada, B. Impacts of airflows, internal heat and moisture gains on accuracy of modeling energy consumption and indoor parameters in passive building. *Energy Build.* **2013**, *64*, 372–383. [CrossRef]
95. Górzeński, R.; Szymański, M.; Górka, A.; Mróz, T. Airtightness of Buildings in Poland. *Int. J. Vent.* **2014**, *12*, 391–400. [CrossRef]
96. Basińska, M.; Koczyk, H. Analysis of the possibilities to achieve the low energy residential buildings standards. *Technol. Econ. Dev. Econ.* **2016**, *22*, 830–849. [CrossRef]

97. Sikora, M.; Siwek, K. Energy audit of the residential building. *J. Mech. Energy Eng.* **2018**, *2*, 317–328. [CrossRef]
98. Ordinance of the Minister of Infrastructure of 12 April 2002 (As Amended) on Technical Conditions to Be Met by Buildings and Their Location. Journal of Laws. No. 75, Item 690 (As Amended). Available online: https://isap.sejm.gov.pl/isap.nsf/DocDetails.xsp?id=WDU20020750690 (accessed on 14 April 2021).
99. Krawczyk, D.A. Analysis of Energy Consumption for Heating in a Residential House in Poland. *Energy Procedia* **2016**, *95*, 216–222. [CrossRef]
100. Piotrowska, E.; Borchert, A. Energy consumption of buildings depends on the daylight. *E3S Web Conf.* **2017**, *14*, 01029. [CrossRef]
101. Hałacz, J.; Skotnicka-Siepsiak, A.; Neugebauer, M. Assessment of Reducing Pollutant Emissions in Selected Heating and Ventilation Systems in Single-Family Houses. *Energies* **2020**, *13*, 1224. [CrossRef]